APS physics

CHORUS

This is the accepted manuscript made available via CHORUS. The article has been published as:

Fission barriers at the end of the chart of the nuclides

Peter Möller, Arnold J. Sierk, Takatoshi Ichikawa, Akira Iwamoto, and Matthew Mumpower

Phys. Rev. C **91**, 024310 — Published 12 February 2015

DOI: 10.1103/PhysRevC.91.024310

LA-UR-14-24999

Fission barriers at the end of the chart of the nuclides

Peter Möller,[1,*] Arnold J. Sierk,[1] Takatoshi Ichikawa,[2] Akira Iwamoto,[3] and Matthew Mumpower[4]

[1] *Theoretical Division, Los Alamos National Laboratory, Los Alamos, New Mexico 87545, USA*
[2] *Yukawa Institute for Theoretical Physics, Kyoto University, Kyoto 606-8502, Japan*
[3] *Advanced Science Research Center, Japan Atomic Energy Agency (JAEA), Tokai-mura, Naka-gun, Ibaraki, 319-1195, Japan*
[4] *Joint Institute for Nuclear Astrophysics, University of Notre Dame, 225 Nieuwland Science Hall, Notre Dame, IN 46556, USA*

We present calculated fission-barrier heights for 5239 nuclides, for all nuclei between the proton and neutron drip lines with $171 \leq A \leq 330$. The barriers are calculated in the macroscopic-microscopic finite-range liquid-drop model (FRLDM) with a 2002 set of macroscopic-model parameters. The saddle-point energies are determined from potential-energy surfaces based on more than five million different shapes, defined by five deformation parameters in the three-quadratic-surface shape parameterization: elongation, neck diameter, left-fragment spheroidal deformation, right-fragment spheroidal deformation, and nascent-fragment mass asymmetry. The energy of the ground state is determined by calculating the lowest-energy configuration in both the Nilsson perturbed-spheroid (ϵ) and in the spherical-harmonic (β) parameterizations, including axially asymmetric deformations. The lower of the two results (correcting for zero-point motion) is defined as the ground-state energy. The effect of axial asymmetry on the inner barrier peak is calculated in the (ϵ, γ) parameterization. We have earlier benchmarked our calculated barrier heights to experimentally extracted barrier parameters and found average agreement to about one MeV for known data across the nuclear chart. Here we do additional benchmarks and investigate the qualitative, and when possible, quantitative agreement and/or consistency with data on β-delayed fission, isotope generation along prompt-neutron-capture chains in nuclear-weapons tests, and superheavy-element stability. These studies all indicate that the model is realistic at considerable distances in Z and N from the region of nuclei where its parameters were determined.

PACS numbers: 24.75.+i,25.85.Ec,26.30.Hj,21.60.n

* moller@lanl.gov

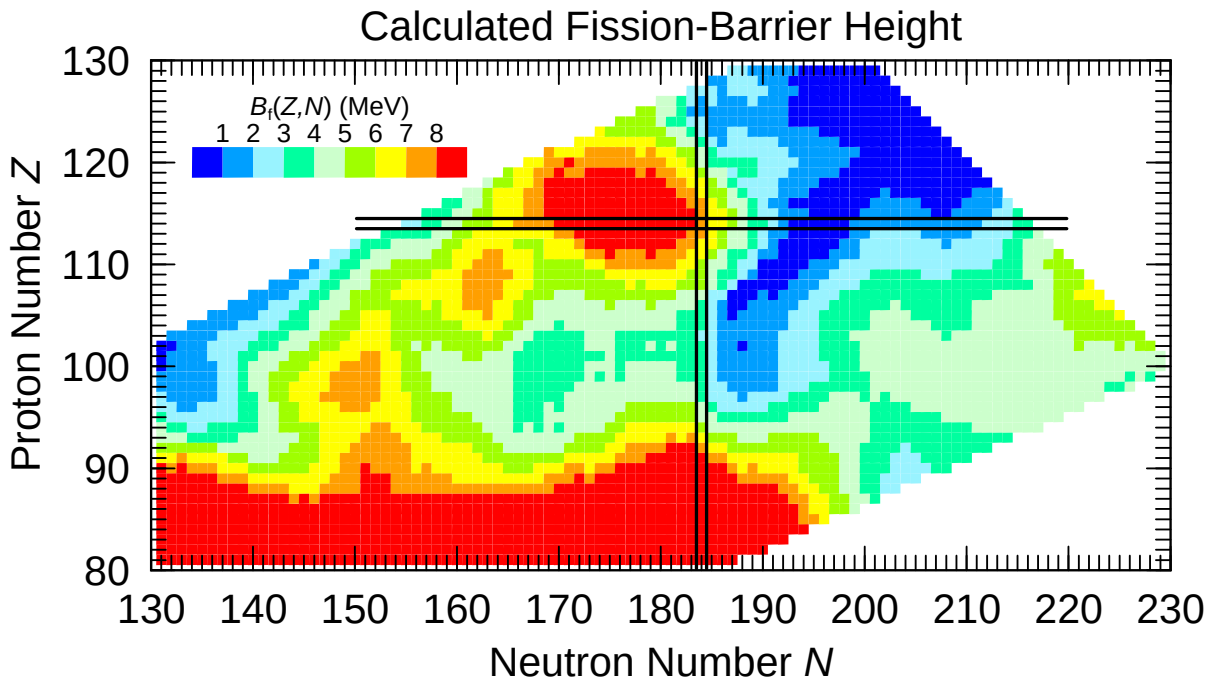

FIG. 1. (Color online) Calculated fission-barrier heights for 3282 nuclei. The highly variable structure is mostly due to ground-state shell effects. Ground-state shell effects are particularly strong in the deformed regions around $^{252}_{100}\mathrm{Fm}_{152}$ and $^{270}_{108}\mathrm{Hs}_{162}$ and in the nearly spherical region near the next doubly-magic nuclide postulated to be at $^{298}_{114}\mathrm{Fl}_{184}$. Our strongest shell effects are slightly offset to the left with respect to this isotope.

I. INTRODUCTION

In actinide fission a nucleus typically evolves from a single nucleus in its deformed ground state to two separated fragments: one large roughly spherical fragment with nucleon number $A \approx 140$ and a smaller deformed fragment with the remainder of the nucleons. In Ref. [1] we presented calculations of fission potential-energy surfaces and associated barrier heights for 1585 nuclei, and some conclusions based on these studies. We now extend the study and tabulate barriers for 5239 nuclides in the region $171 \leq A \leq 330$ for all nuclei between the proton and neutron drip lines. All aspects of the calculations are identical to those presented in Ref. [1] where full details are given. However, we review both some important ingredients and features of our approach and how it is positioned with respect to other fission-barrier calculations. An overview of the results is presented in Figs. 1 and 2.

We have previously made the case that to study the nuclear potential energy during the shape evolution in fission and to allow the nucleus freedom to evolve into fragments with different shapes and into different fragment mass divisions, it is necessary to calculate the nuclear potential energy as a function of, at a minimum, five shape degrees of freedom corresponding to: elongation, neck radius, left fragment shape, right fragment shape and the asymmetry of the mass division [1, 3–6]. It is also necessary to space the deformation points fairly densely so that shell-structure features appear accurately in the calculated potential-energy surfaces. As an example, consider the shell-structure effects in the tin-like fragment with $A \approx 140$. In ground-state mass calculations in which the associated microscopic corrections are also tabulated, for example in the FRDM(1992) mass calculation [7] we find that the ground-state microscopic corrections for $^{132}_{50}\mathrm{Sn}_{82}$, $^{130}_{50}\mathrm{Sn}_{80}$, and $^{130}_{48}\mathrm{Cd}_{82}$ are -11.55 MeV, -9.14 MeV, and -9.85 MeV, respectively. Thus, near magic numbers a change by one nucleon changes the microscopic correction by about 1 MeV. See Ref. [7] for precise definitions of the shell-plus-pairing correction, and the associated microscopic correction. The latter quantity is a sum of the shell-plus-pairing correction, the deformation change of the macroscopic energy relative to the sphere and a zero-point energy. We therefore space our asymmetry coordinate so that one step in the asymmetry coordinate corresponds to moving about one proton and one neutron from one fragment to the other. For example, for an $A = 200$ nucleus the symmetric configuration obviously corresponds to a mass division $M_\mathrm{H}/M_\mathrm{L} = 100/100$ and our next grid point in the asymmetry coordinate corresponds to $M_\mathrm{H}/M_\mathrm{L} = 102/98$ where M_H is the heavy-fragment mass and M_L is the light-fragment mass. To allow studies of cold-fusion heavy-ion reactions on $^{208}_{82}\mathrm{Pb}_{126}$ targets leading to superheavy elements, we use 35 grid points in the asymmetry coordinate [1]. In the elongation coordinate Q_2 we use 45 grid points; in the remaining three deformation coordinates, 15 in each. This leads to more than 5 000 000 shapes.

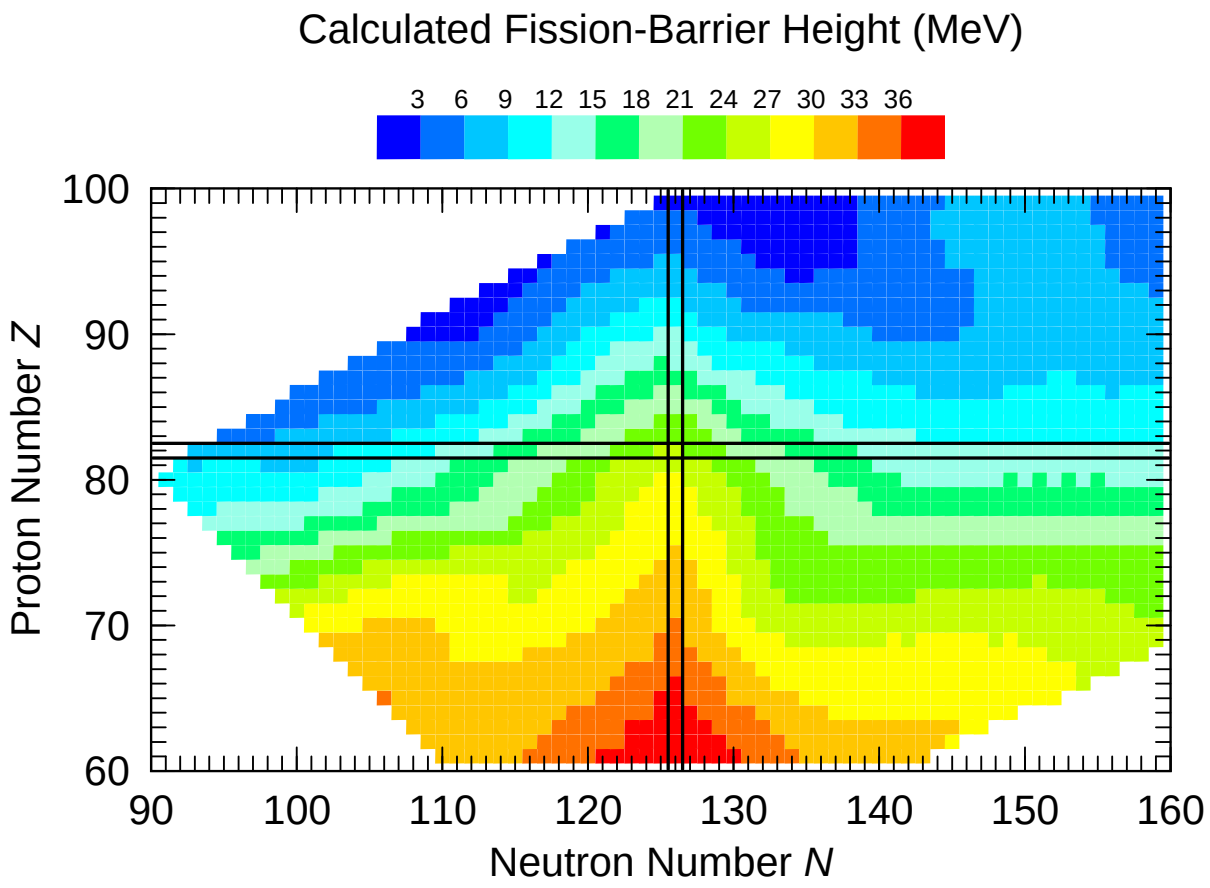

FIG. 2. (Color online) Calculated fission-barrier heights for 2113 nuclei with generally lower proton and neutron numbers than those in Fig. 1. Because the macroscopic energy contributes the major part of the fission-barrier height for most nuclei in this region, and because of the different energy scale compared to Fig. 1, the only shell effects clearly visible come from the $N = 126$ spherical neutron shell.

It should be obvious, but is perhaps not immediately intuitively clear that the consequence is large data storage needs. If the energies for each shape for each of the about 5000 nuclei is stored as a 10 digit number this means that the total data storage space needed is $5\,000\,000 \times 10 \times 5\,000 = 2.5 \times 10^{11}$ bytes, that is 250 Gb of storage. When we started this type of calculation based on millions of shapes in 1999, [3], this was indeed a problem; now it is not.

II. OTHER FISSION POTENTIAL-ENERGY CALCULATIONS

In most previous fission studies various schemes were employed to avoid calculating a complete "hypercube" in all the deformation variables considered. Such complete calculations were impractical until computer performance had evolved sufficiently, roughly achieved around 1995–2000. In macroscopic-microscopic calculations it was the norm to plot energies versus two shape variables, for example β_2 and β_3 (quadrupole and octupole deformations) and "minimize" the potential energy with respect to additional multipoles; typical examples are Refs. [8, 9]. Although such approaches intuitively seem promising, there are significant concerns about the uniqueness and stability of such results. First, when minimizations are carried out at a specific location (β_2, β_3), what are the starting values of the additional shape variables over which the minimization is carried out? A trivial suggestion is that the values obtained for a previous point be used, but which is the "previous point" will depend upon the sequence in which the grid points are considered. It is easy to visualize a surface, even in two dimensions, for which a different result may be found by approaching a particular point from opposite directions. Another strategy could be that the minimizations are started at the value zero of the additional variables at each point (β_2, β_3), but these approaches would miss possible multiple deformed minima. And, even if found, it would be impossible to display multiple minima versus the "hidden" shape variables in a two-dimensional contour plot. Furthermore, none of these methods, which only access a limited

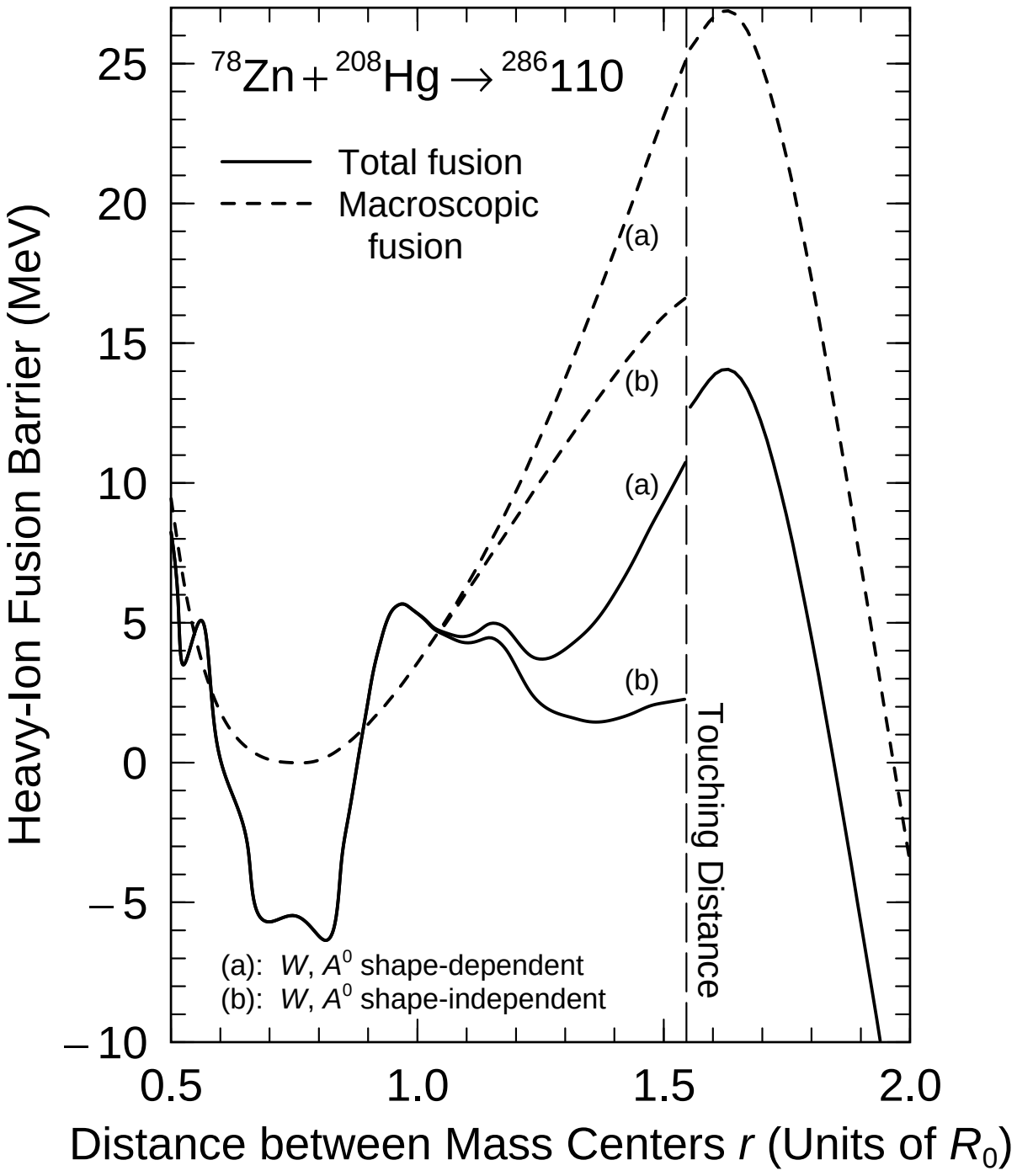

FIG. 3. Calculated macroscopic and total potential energies, for shape sequences leading to the touching configuration, at the long-dashed line, of spherical ^{78}Zn and ^{208}Hg. To the left the calculations trace the energy for a *single, joined* shape configuration, from oblate shapes through the spherical shape at $r = 0.75$ to the touching configuration at $r = 1.52$; to the right the calculations give the energy for separated spherical nuclei beyond the touching point. The continuous path through five-dimensional space from the ground state to the touching configuration is arbitrary; the key point is that the limiting shapes when approaching the line of touching from the left and right are identical, namely spherical ^{78}Zn and ^{208}Hg in contact. At a specific value of r all curves are calculated for the same shape. To obtain continuity of the macroscopic energy at touching, a crucial feature in realistic models, it is essential that various model terms depend appropriately on nuclear shape, as is the case for the curves (a). The slight remaining discontinuity in the *total* fusion energy curve (solid line) arises because the Fermi surfaces of the nuclei readjust at contact, and because pairing and spin-orbit strength parameters also undergo small discontinuous changes there. This figure and caption are adapted from Ref. [2]

part of the higher dimensional space, are guaranteed to find the true saddle points with reasonable accuracy. In some cases, the saddle solutions will be correct, but there is no way to mathematically evaluate the possible errors inside the model framework itself. In many of these minimization studies points that seem near each other in the two-dimensional (β_2, β_3) plots are actually quite distant in the higher-dimensional space. This is often manifested as strong discontinuities appearing in published potential-energy contour diagrams or plots of energy surfaces. Despite these known deficiencies, these methods are still in routine use today [10]. However, very recently other groups previously employing such approximations have come to the conclusion that the minimization method is deficient, not just in principle but also in practice. In one recent macroscopic-microscopic model study, the calculations were carried out for complete multidimensional "hypercubes" and confirmed that the immersion methods we employ are crucial to avoiding spurious results from the use of minimization. It is stated directly *"This shows that the minimization is an uncertain method of the search for saddles ..."* in the summary conclusions [11]. This study also directly contradicts large axial asymmetry effects found at fission saddle points with essentially the same macroscopic-microscopic model by use of minimization in Ref. [10].

Currently, the main alternative approach to macroscopic-microscopic calculations of fission-barrier potential-energy surfaces and saddle points is the constrained Hartree-Fock method introduced in 1973 [12]. Those authors state *"One of the advantages of this type of calculation is that deformation energy curves can be calculated without making a complete map of the deformation energy surface"*. Another comment that is often made in connection with determining fission saddle points is that "constrained selfconsistent methods automatically take all higher shape degrees of freedom into account". However, these statements are misleading. Imposing shape constraints in selfconsistent methods is mathematically equivalent to the use of minimization techniques in macroscopic-microscopic methods, which we, and now other groups, have demonstrated are flawed. A detailed discussion is in Ref. [1]. A very transparent discussion coming from outside the field of nuclear physics is in Ref. [13]. The example used there is the determination of the Continental Divide in the United States, but the problem is essentially identical to that of finding saddle points in potential-energy surfaces, although easier to visualize because geographical topography is studied in 2D spaces only.

It has been suggested that when constrained HF or HFB calculations are presented, for example as two-dimensional contour maps a *necessary* condition to impose on the results is that the spatial overlap between the wave-functions for neighboring grid points in the contour plot should be large. If there exist neighbor points that do not fulfill a required overlap criterion, then one would need to go from 2 to 3 constraints, or in the general case add one additional constraint and again impose the continuity check [14]. But even if the potential energy obtained with two constraints corresponds to a continuous variation of the densities, it is by no means certain a saddle point on this surface is a good approximation to the real (lowest) saddle point, see for example the discussion of figure 5 in Ref. [1]. Based on these observations of problems with existing alternative methods and the evidence from our multitude of benchmarks, see below, we feel that the approach we use is the most accurate currently available for large-scale calculations of databases of various fission-barrier properties.

III. SUMMARY OF ESSENTIAL MODEL FEATURES

In the macroscopic-microscopic model the energy for a specific, prescribed nuclear shape is calculated as a sum of a macroscopic energy and a microscopic shell-plus pairing correction. In the community, several different models are used for the macroscopic and the microscopic parts. For example, the microscopic part can be based on a modified-oscillator (Nilsson) single-particle potential [15, 16], a Woods-Saxon single-particle potential [17], a folded-Yukawa single-particle potential [18], and others. We use what we have called the finite-range liquid-drop model (FRLDM) [19] for the macroscopic part and the folded-Yukawa single-particle model as the starting point for the microscopic part. When we refer to the full macroscopic-microscopic model, we for brevity use the notation FRLDM when the macroscopic part is the finite-range liquid-drop model and FRDM when the macroscopic part is based on the finite-range droplet model; we do not use the latter in our fission-barrier calculations, for reasons we explain below.

A. Macroscopic model

For the macroscopic energy we use the finite-range liquid-drop model (FRLDM). Briefly stated, it is based on a standard shape-dependent "liquid-drop" model [20, 21], which is enhanced to take the finite range of the nuclear force [19] and the diffuseness of the charge distribution [22] into account. In the original liquid-drop model, the surface energy is strictly proportional to the surface area of the nucleus [23]. For shapes with well-developed small-radius necks, this leads to too high a surface-energy contribution to the macroscopic energy in the neck region. For such shapes the finite range of the attractive nuclear force may be thought of as reaching across the neck region to nucleons on the opposite side of the neck, leading to a reduction of the surface energy. The effect is also important

in calculations of heavy-ion interaction barriers and even for some ground-state shapes containing higher-multipole components. An in-depth presentation of the model and discussions of these issues are found in Refs. [7, 19, 22].

When fission was discovered [24], it was realized that the observations could be interpreted in terms of a macroscopic, deformable liquid-drop model [25, 26]. Bohr and Wheeler very soon afterward presented a quantitative description of the shape dependence of the surface and Coulomb energies in terms of Taylor expansions and obtained the systematics of fission-barrier heights for nuclei throughout the periodic system [23].

To model nuclear masses more accurately than was possible with the original liquid-drop model, or semi-empirical mass model [27], phenomenological shell corrections with adjustable parameters were often added to the macroscopic expression. In these studies it was observed that in addition to a strong contribution from microscopic effects at and near magic numbers, it was necessary to account for the extra binding that was observed for nuclei with equal or nearly equal proton and neutron numbers [20]. One commonly used form for this "Wigner energy", which we use, is

$$E_{\rm W} = W \left[\frac{|N-Z|}{N+Z} \right], \tag{1}$$

where for the Wigner constant W, we use the value 30 MeV. In nuclear mass models this term was customarily included without a shape dependence. For a ^{236}U nucleus this contribution to the nuclear potential energy is 6.6 MeV. However, if we use the model to describe the highly-deformed shapes in fission near the transition from a single shape to two fragments, it is relevant to ask if this shape-independent formulation makes sense. For example, for the simple case of two touching spheres we would hope to get the same calculated energy if we consider the system as one very deformed single shape, or as two separate touching nuclei. Clearly, if we consider any division of the original nuclear system with proton and neutron numbers $Z_{\rm comp}$ and $N_{\rm comp}$ into two fragments (1) and (2) with proton and neutron numbers Z_1, N_1, Z_2, and N_2 while preserving neutron–proton asymmetry, that is

$$\begin{aligned} Z_1 &= \alpha \times Z_{\rm comp} \quad N_1 = \alpha \times N_{\rm comp} \\ &\text{and} \\ Z_2 &= (1-\alpha) \times Z_{\rm comp} \quad N_2 = (1-\alpha) \times N_{\rm comp} \end{aligned}$$

where α is a fractional number in the range 0–1, then there will be a Wigner energy contribution $E_{\rm W} = 6.6$ MeV to each of the touching nuclei. Thus for the touching configuration there will be a difference 6.6 MeV in calculated potential energy if it is treated as a scission configuration or as two touching nuclei. Obviously, for the touching configuration one would also need to take into account the interaction energies between the two nuclei. After doing this, to avoid this 6.6 MeV remaining discontinuity, it is necessary to introduce a shape dependence for the Wigner energy, so that

$$E_{\rm W} = W \left[\frac{|N-Z|}{N+Z} \right] B_{\rm W}, \tag{2}$$

where the shape-dependent function $B_{\rm W}$ evolves continuously from $B_{\rm W} = 1$ for a shape with no discernible neck to $B_{\rm W} = 2$ as the shape evolves into separated fragments. These issues are further discussed in [28] where the exact expression we use for the deformation dependence of $B_{\rm W}$ is given. The specific functional form for this dependence is not derived, but is arbitrarily defined to smoothly transition from a value of 1 to a value of 2 as a function of the developing neck. Similar considerations show that it is necessary to introduce a shape dependence for the constant, "$a_o A^0$ term", that occurs in the FRLDM. The FRLDM used in our calculations is completely specified in [7] in section 3.5, except that the above shape dependencies were not introduced. Thus the constant and Wigner terms in Eq. (62) in [7] are generalized to

$$\begin{aligned} &E_{\rm macr}(Z,N,\text{shape}) = \ldots \\ &+ a_0 A^0 B_{\rm W} \\ &+ W \left(|I| B_{\rm W} + \left\{ \begin{array}{ll} 1/A & , \ Z \text{ and } N \text{ odd and equal} \\ 0 & , \ \text{otherwise} \end{array} \right. \right) \\ &\quad \ldots \end{aligned} \tag{3}$$

Potential-energy calculations without and with these shape-dependencies are shown in Fig. 3. The slight discontinuity in the "Total fusion" curve is mainly due to the equalization of the Fermi surfaces of the two colliding nuclei that occurs after contact.

Because, in our studies since the year 1999, we have calculated fission potential-energy surfaces for several million deformation-grid points, this has systematically lowered all calculated fission saddle-point energies compared to those calculated previously using a much smaller space of shapes. The macroscopic-model constants thus had to be readjusted by a simultaneous fit to experimental barrier heights and ground-state masses, leading to different macroscopic parameters from those in [7], referred to as FRLDM(1992). We now use the constants FRLDM(2002), given in Ref. [2].

We emphasize that in nuclear mass calculations we obtain the most accurate results by use of the finite-range droplet model (FRDM). This model is a combination of the FRLDM and the droplet model [29], which allows, at a macroscopic level, calculation of effects of Coulomb redistribution (some charge is pushed from the center toward the surface) and other related effects. These effects lead to about a 15% improvement in mass-model accuracy. But the droplet model enhancement introduces many terms that are derived as expansions in terms of small deformations around a spherical shape. It is therefore not possible to take it to large deformations and make a continuous energy transition at scission to separated shapes using this macroscopic model. Therefore it can not be used in calculations of fission potential-energy surfaces. In our study of masses in Ref. [7] we actually performed a limited calculation of fission-barrier heights in the FRDM and the model parameters were determined by adjusting to a weighted sum of masses and barrier heights. At that time the barrier saddle points were determined from a 1973 calculation [30, 31] in a three-dimensional space containing only 175 different shapes. The saddle shapes obtained in this calculation did not exhibit obvious neck indentations (and as we now realize were not very realistic [3, 4]) so we did not address the issue that the droplet model and the FRDM become increasingly inaccurate at large deformations. This is why we now in fission calculations use only the FRLDM.

B. Microscopic model

The shell-plus-pairing corrections are calculated by use of Strutinsky's method from single-particle levels in a folded-Yukawa potential. The single-particle potential is almost unchanged since 1973 [18, 32], except that in 1980, to permit application to the whole nuclear chart, we let the neutron and proton spin-orbit strengths depend weakly on the nucleon number A [33]. The shell-plus-pairing corrections are calculated as described in [18] with the following enhancements. First, to avoid the well-known collapses of the BCS method, we now use a Lipkin-Nogami pairing model implemented as explained in detail in [34]. Again, imposing continuity at scission required that some constants of the Strutinsky and pairing models depend on deformation, which is discussed in detail in [7, 28]. Full details of the current implementation of the microscopic model are given in Ref. [7], including values of all its constants and various shape dependencies, if any.

C. Deformation grid

Although many of the essential features of the macroscopic-microscopic model were developed up to 40 years ago, it is the continuous increase in computer power that has made it possible to exploit its full potential. In calculations 40 years ago, theoretical studies of mass asymmetry in fission had to be based on potential-energy surfaces calculated for only for a very few shapes: for example versus two independent deformation coordinates for 20 shapes in an early (1970) study [35] versus 3 independent shape coordinates for 175 shapes in 1973 [30]. The 1973 calculation took about 30 hours on a CDC 6600, at Los Alamos Scientific Laboratory, a computer shared by hundreds of researchers. Both these (and other) calculations obtained mass-asymmetric outer saddle points but beyond the outer saddles the potential-energy contour plots developed the deepest "valley" for shapes corresponding to symmetric divisions, in apparent contradiction to experimentally observed asymmetric fragment splits. These results were dismissed by comments like "valleys are not invariant under coordinate transformation" [30] (an observation originally emphasized by Wilets [36]) or, that dynamics determined the final outcome. However, the asymmetry in actinide fission was almost since its discovery explained in a hand-waving fashion as due to a preference of the system to divide into one fragment as close as possible to the spherical, doubly-magic ^{132}Sn nucleus and a remainder, a smaller, deformed fragment. Thus, to permit the potential energy to contain all deformation features related to such divisions one needs to calculate the potential, as stated previously, versus at least five shape degrees of freedom: elongation, neck radius, the two nascent-fragment shapes, and mass asymmetry. In the three-quadratic-surface parameterization one can by suitable manipulations of the expressions involved, see Ref. [1], use these variables, which have an obvious intuitive interpretation, to specify the deformation grid. Also, in this grid the five different shape coordinates are, loosely speaking, nearly orthogonal, which permits a quick, intuitive interpretation of the calculated 5-dimensional potential-energy surfaces. Recently we have also shown that calculations of fission-fragment yields based on a simple "random walk" in this 5D space and the Metropolis algorithm gives excellent agreement with experimental data [37–39]. This

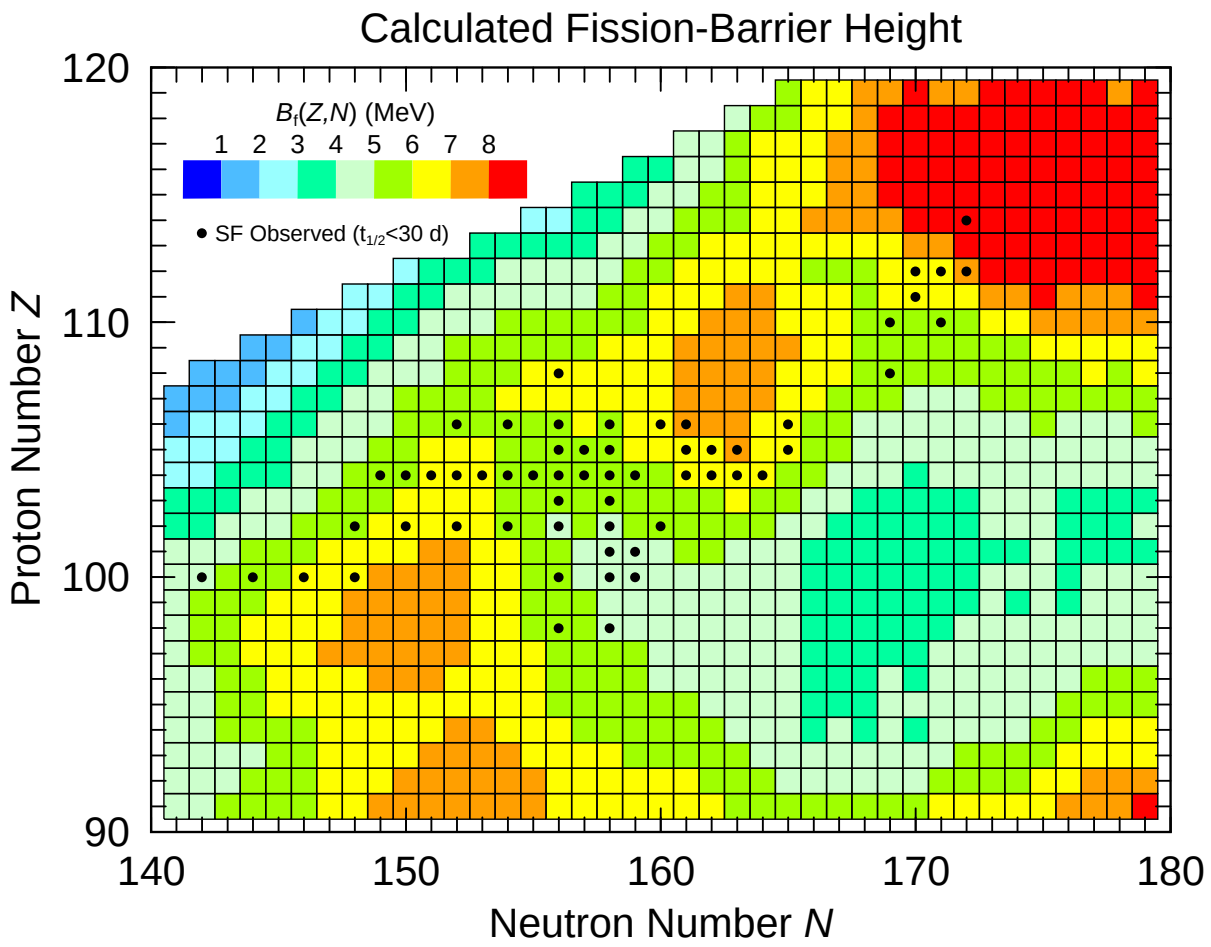

FIG. 4. (Color online) A more detailed look at fission-barrier heights for 980 nuclei in the heaviest region. We have marked with black dots those nuclides for which spontaneous fission with a half-life under about 30 days has been observed.

suggests two conclusions. First, the coordinate choice and spacing is quite consistent with intuitive interpretations; otherwise it would not have been possible to interpret in a straightforward fashion the features of the potential-energy surface in terms of symmetric and asymmetric valleys, different saddle points leading into these different valleys, and ridges in between [1, 6], nor would the Metropolis algorithm have given as realistic results as it now does. Second, we can conclude, because the yield calculations reproduce the substantial differences between the ^{236}U and ^{240}Pu yields [37] that the calculated potential energy is realistic also beyond the outer saddle points, which had not been clearly established earlier, although some hints had been seen in calculations of the most-probable mass divisions [6]. The algebra that is involved in taking the above intuitive coordinate concepts into the actual expressions that in the three-quadratic-surface parameterization generate these shapes is rather tedious and we therefore direct the reader to Ref. [1] for details.

Axially asymmetric deformations are also investigated, but these studies are limited to the ground state and the inner-barrier saddle point. Since the three-quadratic-surface shapes are not able to generate optimal ground-state shapes for some nuclei we have furthermore calculated ground-state energies in the ϵ and β parameterizations. Again, the precise definitions of the deformation grids in these three additional potential-energy calculations are given in Ref. [1], where also details on how the barrier heights are extracted based on the combined information contained in these four complementary potential-energy surfaces are given.

IV. RESULTS

We have calculated barrier heights B_f for 5239 nuclides exactly as described in Ref. [1] and references cited therein. We have summarized the model features in the section above, in particular facts and features that might be somewhat

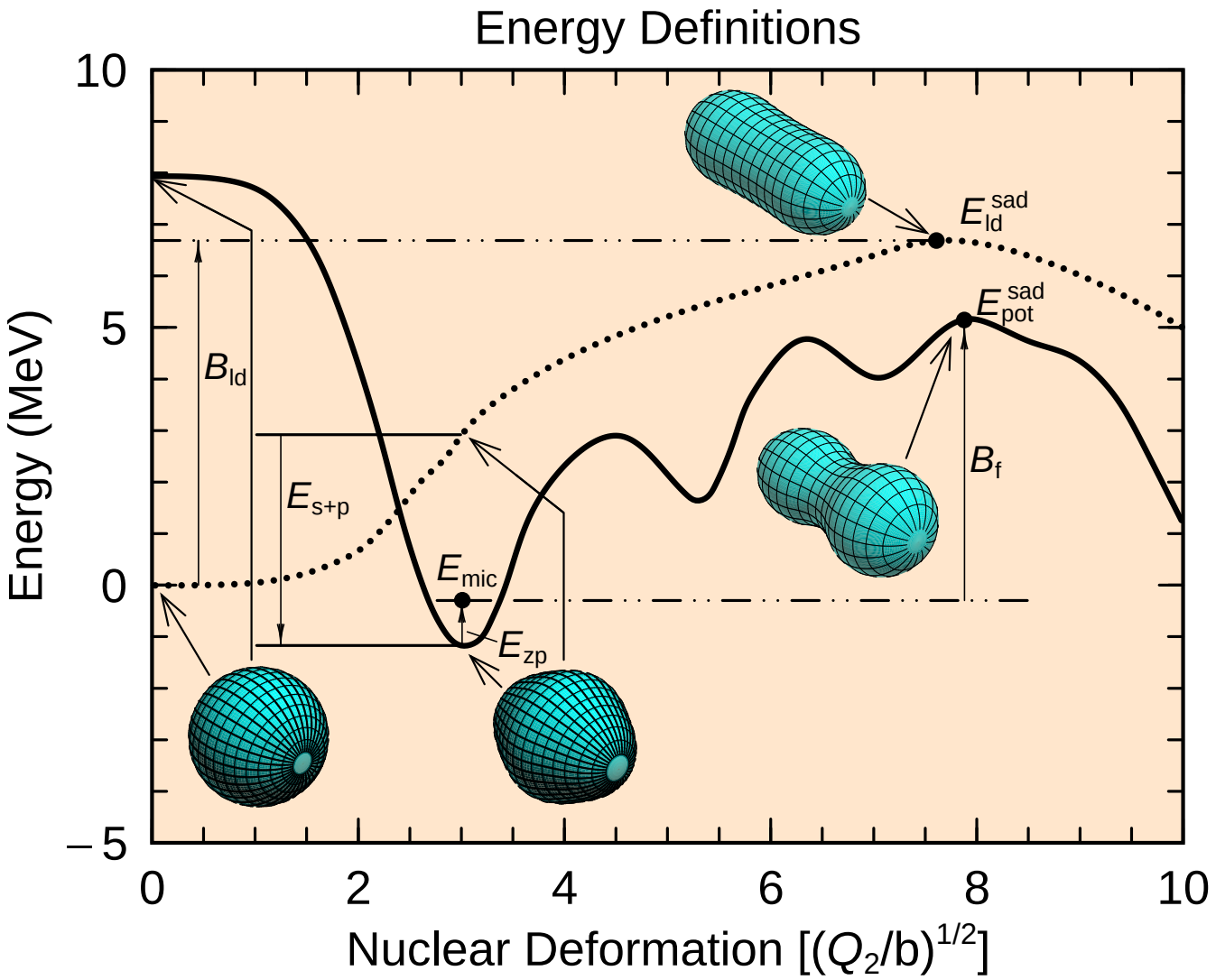

FIG. 5. (Color online) Various energy concepts used in macroscopic-microscopic fission potential-energy calculations. The dotted line is the macroscopic "liquid-drop" energy along a specified path; the solid line is the total macroscopic-microscopic energy along a partially different shape sequence. So that the various energy concepts can be illustrated, the shapes for which the energies have been calculated are: At $Q_2 = 0$ the energies are calculated for a spherical shape. For the shapes from the sphere to the ground-state shape, the shapes are the same for both curves and chosen so that they evolve continuously from the sphere to the calculated macroscopic-microscopic ground-state shape. From the ground state towards larger deformations the total-energy curve is along the optimal fission path that includes all minima and saddle points identified along this path in the five-dimensional deformation space; the liquid-drop-energy curve joins smoothly the macroscopic energy for the shape at the macroscopic-microscopic ground-state (which is not the lowest macroscopic energy at this value of Q_2) to the liquid-drop-model saddle point. The energies are calculated for ^{232}Th. Some important shapes are also shown.

time consuming to trace in a quick scan of the references. The barriers are tabulated in Table I.

The fission-barrier properties of our model have previously been benchmarked with respect to known data for nuclides near β-stability. We have shown that we reproduce the outer barrier peak height for 31 nuclides from $^{70}_{34}\mathrm{Se}_{36}$ to $^{252}_{98}\mathrm{Cf}_{154}$ with an rms deviation of only 1.0 MeV [2]. We have also compared calculated actinide inner and outer barrier heights as well as the height of the fission-isomer minimum to barrier parameters extracted from various types of experimental data, often cross sections as functions of energy for neutron-induced fission [1]. In this context we observe that the "experimental" barrier parameters are not as directly measured data as, for example, nuclear masses are in some experiments. The "experimental" barrier parameters are numbers occurring in models of experimental cross sections. Moreover, these models almost always assume one-dimensional barriers whereas our barrier parameters refer to saddles and minima in five-dimensional deformation spaces. Further complicating the situation is that different evaluations (of different sets of experimental data, and/or just using different cross-section

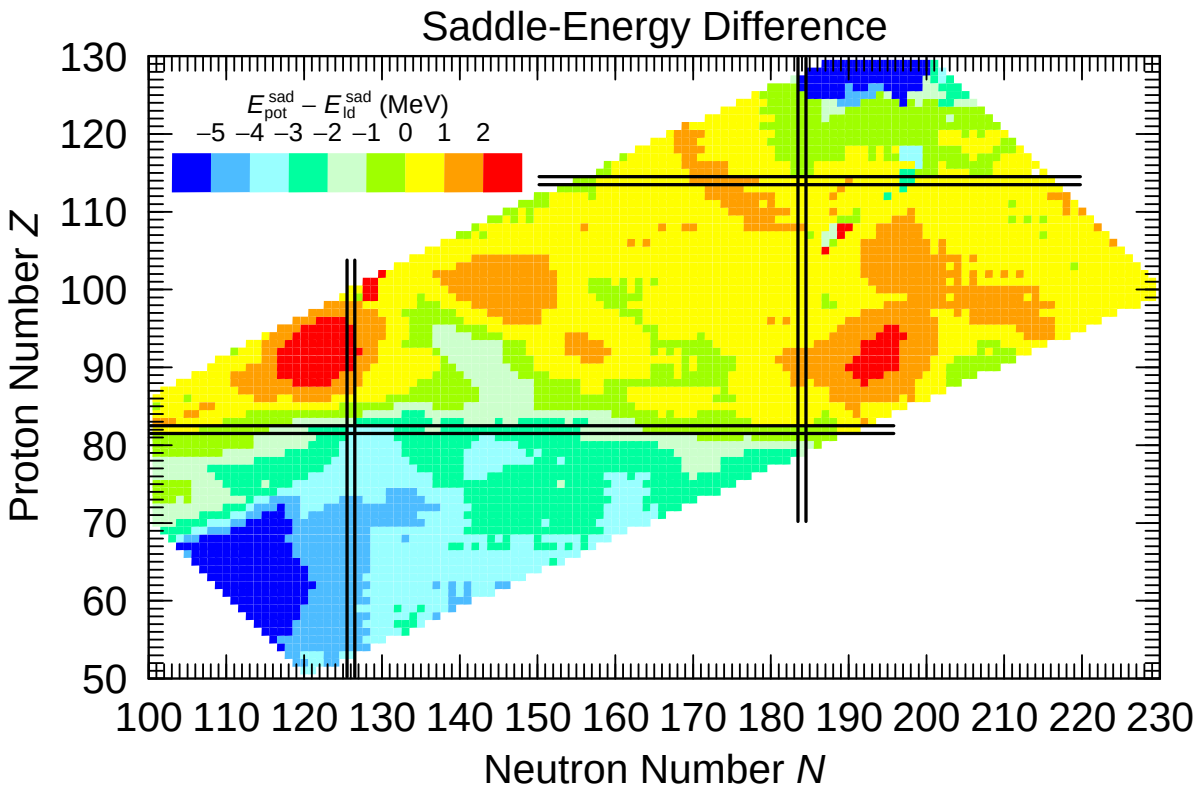

FIG. 6. (Color online) Difference between the saddle-point energy obtained from the five-dimensional macroscopic-microscopic potential-energy surface and the saddle-point energy obtained from a surface in the same deformation space using only the macroscopic model for 5139 nuclei.

models) often lead to different results for the extracted barrier parameters. For example Blons and collaborators [40] consistently find that the so called "third minima" of some light actinide nuclei are very shallow and no more than 0.5 MeV or so below the surrounding second and third barrier peaks, which are about 6 MeV above the ground-state minimum, in good agreement with results obtained in our current model [41]. In contrast, Csige and collaborators [42–44] find third minima for nuclei in this region that are up to 3 MeV below the surrounding peaks. We find it difficult to reconcile with potential-energy calculations the substantial difference in barrier structure they find between ${}^{232}_{92}U_{140}$ [42] and ${}^{232}_{91}Pa_{141}$ [43] in these studies. A change by just one proton and one neutron cannot, in potential-energy calculations, result in such large differences in barrier structure. For these reasons we refer to Figs. 23–32 in Ref. [1] for a qualitative benchmark of our calculations with respect to barrier parameters derived from analysis of experimental cross sections, rather than relying on a calculation of an rms deviation between our model calculations and model-dependent "experimental" barrier parameters with inherently similar levels of uncertainty. Such quantitative indicators are easy to misuse for a spurious sense of precision.

Barrier heights have also been estimated from electron-capture (EC) delayed fission data; for some recent discussions see [1, 45, 46]. In EC-delayed fission, daughter states up to the electron-capture Q-value $Q_{\rm EC}$ are populated. However phase-space properties result in daughter population probabilities that are roughly proportional to $(Q_{\rm EC} - E^*)^5$ where E^* is the excitation energy above the ground state in the daughter. Therefore the decay intensities to sufficiently high energies so that EC-delayed fission occurs are usually low. For EC-delayed fission to be observable a rough rule of thumb is that

$$Q_{\rm EC} \gtrapprox B_{\rm f} - 2 \ \ {\rm MeV} \tag{4}$$

We show in Fig. 34 and Table V in Ref. [1] the degree to which our calculated masses and fission-barrier heights satisfy this empirical "rule." With the possible exceptions of a couple of nuclei near $N = 150$, all the observed cases of EC-delayed fission are consistent with our model values. As discussed in Ref. [1], this exception probably occurs because the calculated $N = 150$ neutron gap in the single-particle spectrum in our model is somewhat too large, resulting in too low ground-state energies and slightly too high barriers. But in general the relation is well fulfilled in this comparison, which tests the model far from stability, towards the proton-rich side, across the wide region

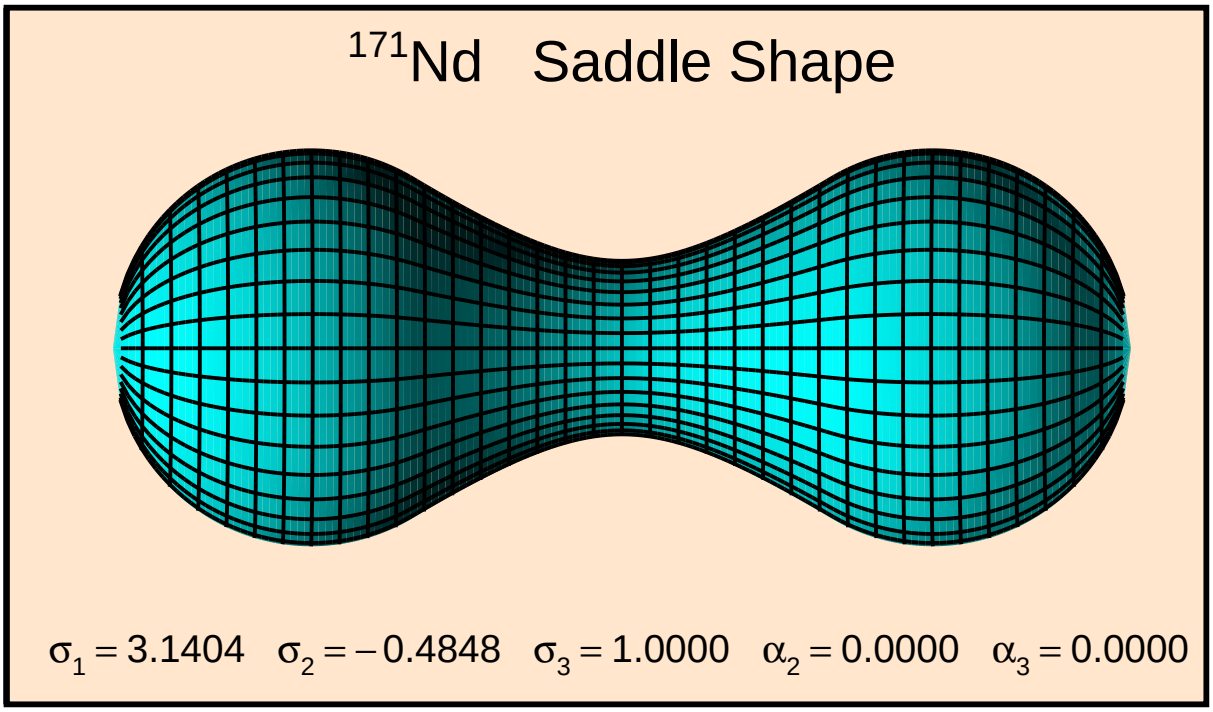

FIG. 7. (Color online) Shape of ${}^{171}_{60}\mathrm{Nd}_{111}$ at the saddle point.

$80 \leq Z \leq 99$ and $100 \leq N \leq 150$.

Calculated barrier heights for 3282 nuclides in the heaviest region are plotted in Fig. 1. Above $Z \approx 100$ the macroscopic contribution to the fission barrier is very low. Therefore survival with respect to spontaneous fission (SF) and the high barriers that are the reason for the long SF half-lives are mainly due to negative ground-state microscopic corrections [47, 48], which can be substantial in some localized regions. We observe such localized regions of high fission barriers in the vicinity of ${}^{252}_{100}\mathrm{Fm}_{152}$, ${}^{270}_{108}\mathrm{Hs}_{162}$, and in the superheavy-element (SHE) region. In our calculations the maximum ground-state microscopic correction occurs at $Z = 116$ and $N = 178$, rather than at $Z = 114$ and $N = 184$ [7]. The regions of high fission barriers coincide with regions of large ground-state microscopic corrections which can exceed (in the negative direction) -6 MeV also for deformed nuclei outside the spherical superheavy region near $Z = 114$ and $N = 184$, namely in the deformed regions centered at ${}^{252}_{100}\mathrm{Fm}_{152}$ and ${}^{270}_{108}\mathrm{Hs}_{162}$. Along the Fm isotope chain the barrier heights decrease rapidly with distance from $N = 152$, and the spontaneous fission half-lives show a similar rapid decrease, which is reproduced in numerous calculations, for example Refs. [28, 49–53].

In Fig. 2 we display calculated barriers for 2113 nuclei for the lighter region in our study. There is less structure here compared to the heavier region in Fig. 1. In this region, the macroscopic energy contributes significantly to the barrier height, leading to the use of a different energy scale in this figure. Therefore, the only easily discernible shell structure is due to the magic neutron number $N = 126$.

For a long time $Z = 99$ as been the upper limit for reasonably accurate experimental fission-barrier parameters [54–57]. Only recently has a barrier height for a heavier system, ${}^{274}\mathrm{Hs}$, been determined [58]. However, spontaneous fission has been observed for many heavier systems. We can use these data to further benchmark our calculated barrier heights. In Fig. 4 we show in more detail a limited set of the data in Fig. 1, namely nuclei from the actinide region up to $Z = 120$. We show as black dots those nuclei for which spontaneous fission has been observed with a half-life less than 30 days, taken from the compilation of Ref. [59]. The aim is to investigate what correlations we find between the calculated barrier heights and the observed fissioning nuclei. This is only to get an overview of the situation because we do not

- show that most nuclei in this plot have not been observed experimentally.
- account for the highly variable effect of specialization energies in odd-even and odd-odd nuclei on spontaneous fission half-lives; this effect can increase half-lives by a factor 10^1 to a factor 10^9 [49].
- account for the branching ratios between α-decay and fission. For example a system may have a spontaneous fission half-life of, say, one second, but SF may still not be observed because the α-decay half-life is in the microsecond range.

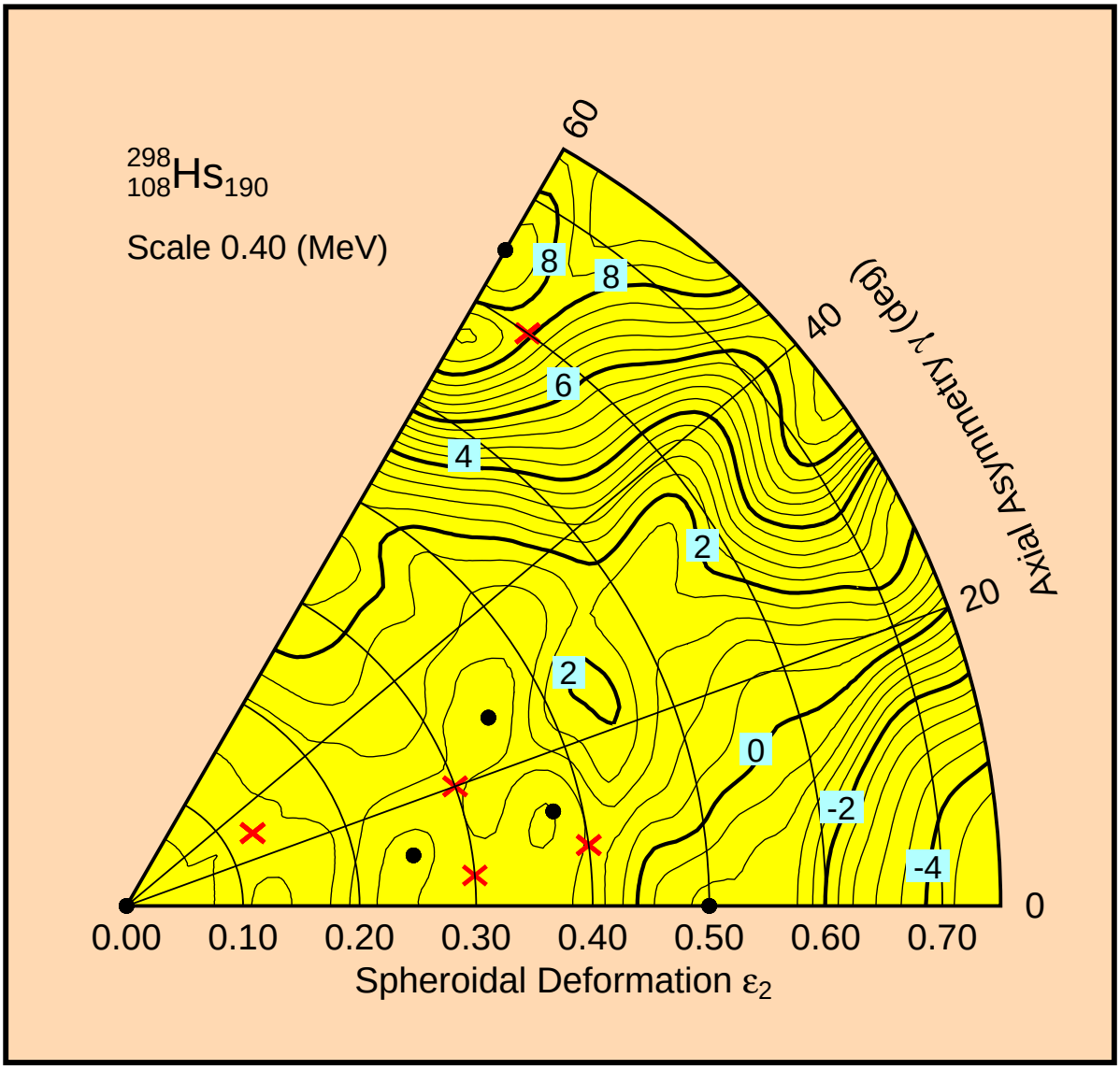

FIG. 8. (Color online) Calculated potential-energy surface for $^{298}_{108}$Hs$_{190}$. Local minima are shown by black dots, while saddle points are shown by magenta-colored crosses. The ground state is located at $\gamma = 60$ and $\epsilon_2 = 0.65$, because this is the minimum with the highest barrier with respect to fission, see text for further discussion. But with such a low barrier this isotope would not be observable.

Despite these limitations we see some interesting correlations that support the accuracy of the calculated barriers. SF is almost exclusively observed in the regions where the predicted barrier is between slightly below 5 MeV and 7 MeV, with only 4 exceptions out of 58 data points. So we conclude from these qualitative arguments that our barrier heights are consistent with the observed occurrences of SF in the heavy-element region.

In some calculations of fission barriers, it is assumed that the shell-plus-pairing corrections at the saddle are small and can be neglected, whereas the shell-plus-pairing corrections at the ground states always have to be included. Refs. [47, 48, 60] are some examples of such studies. We test this assumption below. First, we illustrate some concepts by showing in Fig. 5 a few important quantities and definitions. The total potential energy at a specific shape $E_{\rm pot}$ is the liquid-drop-model energy at this specific shape plus, for the same shape, the shell-plus-pairing correction $E_{\rm s+p}$ (which is negative at the ground state in the case here). To obtain manageable numbers we give all energies relative to the spherical liquid-drop energy, including the liquid-drop energy itself. Therefore at a specific deformation β (which is a shorthand for any number of deformation parameters, by definition zero for a sphere)

$$E_{\rm pot}(\beta) = E_{\rm ld}(\beta) + E_{\rm s+p}(\beta) - E_{\rm ld}(\beta = 0) \tag{5}$$

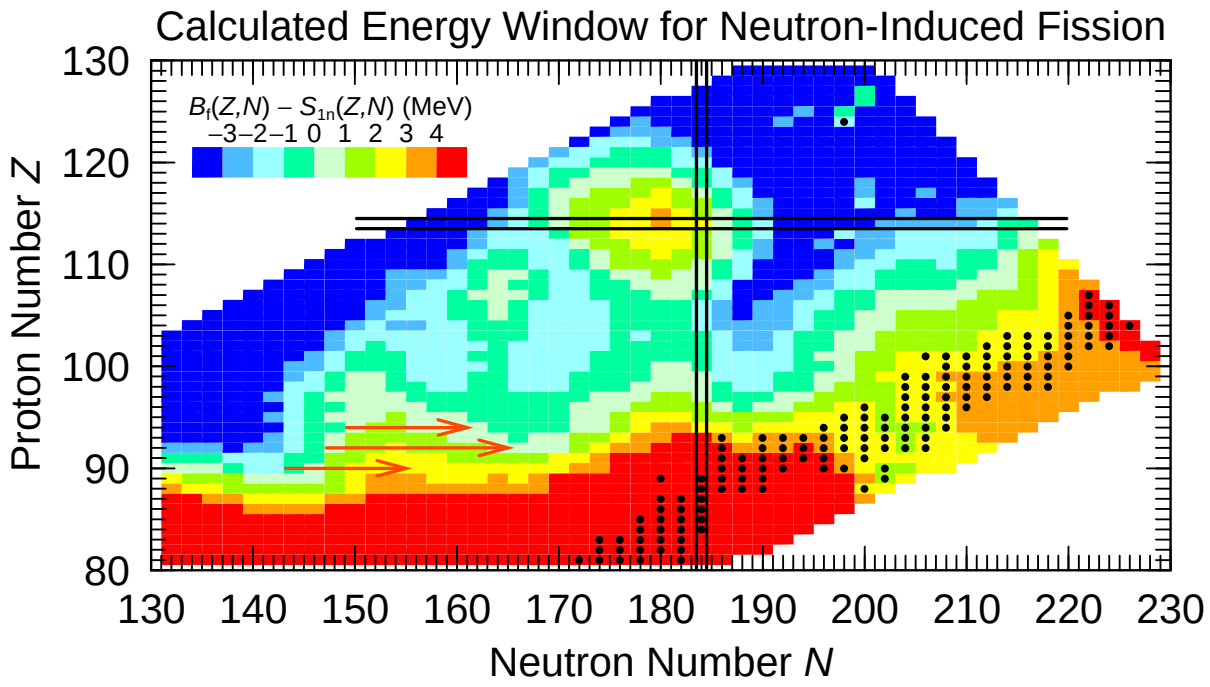

FIG. 9. (Color online) Energy window [7] for neutron-induced fission. The black dots indicate even-N nuclei for which 1.0 MeV $< S_{1n} <$ 2.0 MeV, the so-called r-process boulevard, the region of the chart where the r-process proceeds. If the plotted quantity is negative, the system is unstable with respect to thermal neutron-induced fission. The magenta arrows indicate prompt neutron-capture chains in nuclear weapons tests, see text for further discussion of this and the single outlying dot at $Z = 124$.

The nuclear mass at the ground state is, in our treatment, the sum of $E_{\rm pot}$ at the ground-state minimum and a zero-point energy [33]. Again, this is relative to the spherical liquid-drop mass (or energy) and is often designated "microscopic correction" $E_{\rm mic}$. The "unnormalized" nuclear mass is therefore the spherical liquid-drop mass plus the microscopic correction. It is thus relative to the potential-energy at the ground state **plus** the zero-point energy that we define the barrier height. By accident the macroscopic barrier $B_{\rm ld}$ is, in this example, almost the same as $B_{\rm f}$, but generally this is not the case. For ^{208}Pb the difference would be more than 10 MeV due to the large, negative $E_{\rm s+p}$ at the spherical ground-state shape.

We show in Fig. 6 the differences between our saddle-point energies in the macroscopic-microscopic FRLDM model and the saddle-point energies from our macroscopic FRLDM model, both determined in the same five-dimensional space; of course, the shapes of the saddle points in the two models are different. The difference is, as postulated, fairly small across large regions of the plot. The rms deviation is 2.25 MeV and the mean deviation (with sign) is −0.78 MeV. In the region of large negative deviations, we find the maximum deviation of −8.45 MeV for $^{171}_{60}$Nd$_{111}$. Why does this large deviation occur here? We calculate the shell-plus-pairing corrections at the saddle-point shape and find it is −8.94 MeV. This saddle-point shape is shown in Fig. 7. It is symmetric and the nascent fragments are spherical. The fragments are near doubly-magic $^{78}_{28}$Ni$_{50}$, which in its ground-state has a shell+pairing correction of −5.89 MeV. (As shown in Fig. 5, the *microscopic correction* tabulated in Ref. [7] is different from this number.) Twice this number makes −11.78 MeV. The shell-plus-pairing correction we obtain at the saddle point is close, but slightly smaller for a number of reasons, mainly the shape is not two well-separated Ni nuclei, and the matter in the nascent fragments corresponds to $Z = 26$ and $N = 48$, if the partial spheres are completed to full spheres; the rest of the matter is outside these completed spheres in the neck region. So we now understand why the macroscopic approximation to the saddle energy is of poor accuracy in this particular region. The fragment shell effects dig a deep valley into the potential energy of the compound system in the neighborhood of the saddle point and lower the potential energy by a substantial amount. One may then ask why this does not happen in the actinide region; why does not the shell effect in the doubly-magic $^{132}_{50}$Sn$_{82}$ (which is −12.82 MeV) affect the saddle-point energy in a similar fashion for actinides? The answer is that the saddle shape of $^{171}_{60}$Nd$_{111}$ is much more elongated; $\beta_2 = 2.40$ for this nuclide whereas for $^{232}_{92}$U$_{140}$ and $^{238}_{92}$U$_{146}$ we find that $\beta_2 = 1.06$ and $\beta_2 = 0.86$, respectively. For $^{171}_{60}$Nd$_{111}$ the saddle shape is very close to the configuration of separated fragments so the fragment shell effects are almost fully present at the saddle point, while for actinides, while these effects may be present, they are not able to be as fully

manifested. Also, when the saddle shape is asymmetric, the macroscopic energy is considerably higher than at the macroscopic, mass-symmetric saddle shape, so this increase in the macroscopic energy cancels a considerable fraction of the "fragment" shell effect. When the saddle shape is symmetric, as is the case for $^{171}_{60}\mathrm{Nd}_{111}$ this does not occur so the fragment shell effects are more visible at a symmetric saddle than at asymmetric saddle shapes.

When the barrier is very low seemingly "pathological" results can be obtained. For example we find for $^{298}_{108}\mathrm{Hs}_{190}$ that the plotted difference is 7.90 MeV, a very local, surprising, and large deviation. The macroscopic saddle energy is 0.32 MeV and the saddle energy obtained from the macroscopic-microscopic model is 8.22 MeV. To understand these seemingly incompatible results we show in Fig. 8 the calculated potential-energy surface for $^{298}_{108}\mathrm{Hs}_{190}$, as a function of elongation ϵ_2 and axial asymmetry γ. The details of the calculation and the coordinates are discussed in Ref. [1]. We showed there that for heavy elements one cannot routinely choose as the ground state the lowest minimum in the potential-energy surface because such a minimum may have a very low barrier with respect to fission. Instead one should choose as the ground state the minimum with the highest barrier with respect to fission, which should have the longest half-life. In this case we identify the minimum at $\epsilon_2 = 0.65$ and $\gamma = 60$ with the ground state and the nearby saddle point indicated by crossed lines, with an energy near 8.2 MeV as the "macroscopic-microscopic" saddle point. Thus we seem to get a very large failure of the method to use the macroscopic saddle-point energy instead of the "exact" saddle-point energy. However, a very small perturbation of the calculated energies could result in, say the minimum at $\epsilon_2 = 0.375$ and $\gamma = 15$ to be identified as the most stable minimum, and the nearby saddle at about 0.8 MeV energy to be the macroscopic-microscopic saddle-point energy, now in good agreement with the macroscopic saddle energy. We can summarize these studies as follows

1. When discussing the macroscopic approximation to the saddle energy, it is not meaningful to consider nuclei with fission barriers that are so low they would be too unstable to exist. Fig. 1 shows that most nuclei slightly above $N = 184$ fall in this category, with some interesting exceptions for low Z and large N.

2. Above $Z = 80$ and $N \leq 184$ the rms deviation between the exact and macroscopic model is 1.12 MeV for the 2433 nuclei in this restricted region. The mean deviation is +0.19 MeV. If all nuclei are included the rms deviation is 2.25 MeV and the mean deviation −0.78 MeV, mainly due to the very large negative deviations near $^{171}_{60}\mathrm{Nd}_{111}$.

3. For systems with $Z < 80$ the macroscopic approximation to the saddle potential energy becomes increasingly inaccurate as Z becomes lower.

4. Although the macroscopic saddle energy in some regions is a good approximation to the saddle energy obtained in the macroscopic-microscopic model, the shapes associated with the saddle points are very poor approximations to shapes obtained in realistic models. To model fission properties such as low-energy fission-fragment mass distributions, potential-energy surfaces of at least five dimensions calculated either in a macroscopic-microscopic model or some other model with realistic microscopic shell structure are necessary [37–39].

We desire to investigate the accuracy of the calculated barrier heights for neutron-rich nuclei with the aim of understanding their suitability for use in studies such as fission at the end of the r-process. Unfortunately, there are no large-scale systematic experimental studies of fission properties for large regions of nuclei on the neutron-rich side of β stability. However, some indirect results are available. The r-process can be approximately simulated in certain nuclear explosions through a process called "prompt neutron capture". It is called prompt because the timescale of the neutron fluence is nanoseconds rather than the seconds time scale of the r-process, so the processes are not fully equivalent; no β-decay can occur during the prompt capture due to its short timescale. For a comprehensive discussion of these experiments see Ref. [61]. Because no β-decay takes place during neutron capture the process, with some qualifications [61], proceeds along an isotope chain, successively producing increasingly neutron-rich isotopes of a specific element. One necessary condition for the capture sequence to proceed is that the fission barrier be higher than the neutron-separation energy in the compound system following neutron capture. We investigate if our calculations are consistent with experimental observations as regards this necessary condition. In Fig. 9 we show the difference between calculated barrier heights and calculated neutron-separation energies for even systems. Odd compound systems have a (slightly) higher fission barrier and lower neutron-separation energies so they are irrelevant for locating the termination of the capture sequence. Also shown, with magenta arrows, are the "observed" range of neutron-capture chains on the targets $^{232}_{90}\mathrm{Th}_{142}$, $^{238}_{92}\mathrm{U}_{146}$, and $^{242}_{94}\mathrm{Pu}_{148}$. In the uranium chain $^{257}_{92}\mathrm{U}_{165}$ is reached. This conclusion is not reached by recovering $^{257}_{92}\mathrm{U}_{165}$ in the debris from the explosion, as it has a calculated β-decay half-life of about 0.5 s [62], too short to allow recovery. Rather, one observes higher-Z, less neutron-rich elements at the endpoint of β-decay chains from the original isotopes in the capture chain. The termination point of the neutron-capture chain is deduced from the highest A-value observed in these groups of nuclei.

From Fig. 9 we see that the observed capture chains for the $^{238}_{92}\mathrm{U}_{146}$ and $^{242}_{94}\mathrm{Pu}_{148}$ targets terminate exactly where the plotted function goes below zero, that is, where the fission-barrier height becomes lower than the neutron separation

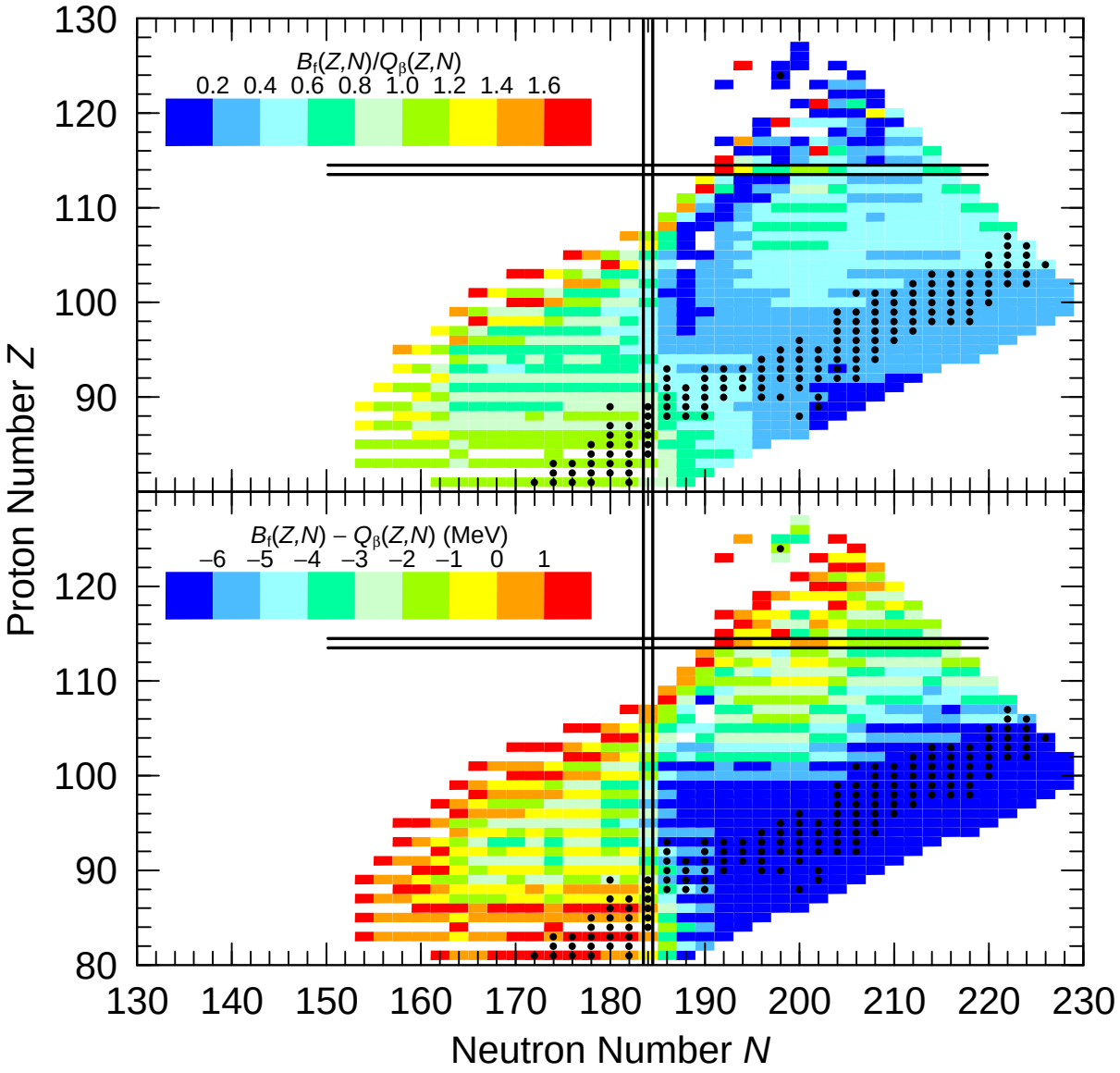

FIG. 10. (Color online) Illustration of quantities affecting β-delayed fission, namely the ratio B_f/Q_β (upper panel) and $B_f - Q_\beta$ (lower panel). Only nuclides for which $B_f - Q_\beta < 2$ MeV are shown. The solid black dots are the same as in Fig. 9, illustrating the "r-process boulevard."

energy, which would result in termination of the capture sequence by fission. Therefore, the calculated results are consistent with these observations. The capture chain on the $^{232}_{90}\mathrm{Th}_{142}$ target terminates before zero is reached, but it is argued [61] that this is because the capture cross sections in this chain are very low. So both our calculated barrier heights and neutron separation energies are consistent with this set of experimental data.

There also could be other mechanisms that cause no nuclei heavier than $A = 257$ to be observed. Nuclei near proton number $Z = 100$ and neutron number $N = 164$ have unusually short half-lives, see [63, 64] for a review and references to original work. The proposed mechanisms for these short half-lives are two-fold: 1) a very thin barrier due to "erosion" of the outer barrier due to the large shell effects associated with two near-doubly-magic fragments in the vicinity of $^{132}_{50}\mathrm{Sn}_{82}$ and 2) effects from the large shell gaps on the mass parameter associated with fission. Both these principles were discussed very early in Ref. [65] and later somewhat more quantitatively in Refs. [6, 28, 66]. Not much data is available for nuclei in this region but we know for Fm there is a sudden drop in half-life 6 nucleons (in this case only neutrons) away from $^{264}_{100}\mathrm{Fm}_{164}$ when we approach this nucleus which corresponds to doubly-magic configurations in both daughter fission fragments in symmetric fission. Since fragment ground-state microscopic corrections near $^{132}_{50}\mathrm{Sn}_{82}$ decrease in a similar fashion with proton and neutron number variation we may as a rule of thumb anticipate

that very short fission half-lives occur at

$$|100 - Z| + |164 - N| \leq 6. \quad (6)$$

Thus even if the actual barriers are higher than the values obtained in our calculations and the capture chain proceeds all the way to $A = 270$ there would be no β-stable products following decay towards stability because the β-decay chains would terminate in fission before relatively stable elements are reached. For instance, suppose $^{260}_{92}\mathrm{U}_{168}$ is reached. When it decays back, according to the above condition $^{260}_{95}\mathrm{Am}_{165}$ would terminate the decay chain by fission. The precursor $^{260}_{94}\mathrm{Pu}_{166}$ has a calculated β-decay half-life of 0.8 s [62], too short to recover this hypothetical isotope.

In Fig. 9 we have marked even-N nuclides with 1 MeV $< S_{1\mathrm{n}} <$ 2 MeV with black dots, defining what is referred to as the r-process boulevard. Along the boulevard the neutron-separation energy is lower than the barrier (although *closer* to stability this is not the case), so according to the results here the r-process can proceed to the heaviest region along this boulevard. However during β-decay back to stability the decay paths will enter regions with very low barriers so some of the nuclides here will have spontaneous fission half-lives in the microsecond range or lower.

We note that the isolated black dot, indicating that the nuclide at $Z = 124$ and $N = 198$ satisfies the condition which defines the "r-process boulevard," is caused by the phenomenon of highly varying deformations of the ground states in neighboring highly unstable isotopes, due to effects similar to those discussed in reference to Fig. 8.

When the β-decay Q_β value is higher than the fission barrier in the daughter, which is the case across a large region of neutron-rich heavy nuclei, β-delayed fission can occur, sometimes with a high probability. This is illustrated in Fig. 10. The ratio between the barrier height and Q_β is shown in the top panel. Only nuclides for which $B_\mathrm{f} - Q_\beta < 2$ MeV are shown, because for decays to energies more than 2 MeV below the barrier peak the delayed fission branch is negligible. Spontaneous fission from the ground state may still occur with a high probability. Smaller ratios correspond to higher probability of delayed fission. As a complementary view we present in the lower panel the magnitude of the energy window for β-delayed fission. However the branching ratio for β-delayed fission is not directly related to the magnitude of this window. For example in a decay with a barrier height of, say, $B_\mathrm{f} = 2$ MeV and $Q_\beta = 6$ MeV the branching ration for delayed fission would normally be much larger than if $B_\mathrm{f} = 6$ MeV and $Q_\beta = 10$ MeV although the energy window for delayed fission is 4 MeV in both of these situations.

In summary, we have benchmarked, both previously and in this work, our potential-energy-surface calculations and associated predicted nuclear properties with respect to

- barrier heights from $^{70}_{34}\mathrm{Se}_{36}$ to $^{252}_{98}\mathrm{Cf}_{154}$ [2],
- nuclear ground-state masses [2],
- actinide "double-humped" fission-barrier parameters [1],
- EC-delayed fission data [1, 45, 46],
- spontaneous-fission properties in the heavy-element region,
- fission-fragment charge-yield data for 70 nuclides [39],
- some prompt neutron-capture data obtained in weapons tests.

These studies have been consistently encouraging and represent quite diverse tests, which show that the calculated potential-energy surfaces give a realistic description of available experimental data, including in regions of the nuclear chart far removed from regions considered in determining the parameters of the model. It therefore seems to be very timely to incorporate this calculated fission-barrier-height data base in studies of fission in the r-process. Such studies would require a sophisticated network that should include pathways and branching ratios for neutron capture, neutron-induced fission, β-decay, β-delayed fission, and spontaneous fission. In the fission branches, ideally the fission-fragment yields should also be included.

This work was supported by travel grants for P.M. to JUSTIPEN (Japan-U.S. Theory Institute for Physics with Exotic Nuclei) under grant number DE-FG02-06ER41407 (U. Tennessee). This work was carried out under the auspices of the National Nuclear Security Administration of the U.S. Department of Energy at Los Alamos National Laboratory under Contract No. DE-AC52-06NA25396. TI was supported in part by MEXT SPIRE and JICFuS and JSPS KAKENHI Grant no. 25287065. MM was supported by the Notre Dame Joint Institute for Nuclear Astrophysics, NSF grant no. PHY0822648.

[1] P. Möller, A. J. Sierk, T. Ichikawa, A. Iwamoto, R. Bengtsson, H. Uhrenholt, and S. Åberg, Phys. Rev. C **79**, 064304 (2009).
[2] P. Möller, A. J. Sierk, and A. Iwamoto, Phys. Rev. Lett. **92**, 072501 (2004).
[3] P. Möller and A. Iwamoto, Proc. Conf. on Nuclear Shapes and Motions. Symposium in Honor of Ray Nix, 25–27 Oct. 1998, Sante Fe, NM, USA Acta Physica Hungarica, New Series, **10**, 241 (1999).
[4] P. Möller and A. Iwamoto, Phys. Rev. C **61**, 047602 (2000).
[5] P. Möller, D. G. Madland, A. J. Sierk, and A. Iwamoto, Tours 2000, Tours Symposium on Nuclear Physics IV, Tours, France September 4–7, 2000, and AIP Conference Proceedings **561**, p. 455 (2001).
[6] P. Möller, D. G. Madland, A. J. Sierk, and A. Iwamoto, Nature **409**, 785 (2001).
[7] P. Möller, J. R. Nix, W. D. Myers, and W. J. Swiatecki, Atomic Data Nucl. Data Tables **59**, 185 (1995).
[8] S. Ćwiok, W Nazarewicz, J. X. Saladin, W. Plociennik, A. Johnson, Phys. Lett. **B322**, 304 (1994).
[9] G. M. Ter-Akopian, J. H. Hamilton, Y. T. Oganessian, A. V. Daniel, J. Kormicki, A. V.Ramayya, G. S. Popeko, B. R. S. Babu, Q. H. Lu, K. Butlermoore, W. C. Ma, S. Ćwiok, W. Nazarewicz, J. K. Deng, D.. Shi, J. Kliman, M. Morhac, J. D. Cole, R. Aryaeinejad, N. R. Johnson, I. Y. Lee, F. K. McGowan, J. X. Saladin, Phys. Rev. Lett. **77**, 32 (1996).
[10] A. Sobiczewski, P. Jachimowicz, and M. Kowal, Int. J. Mod. Phys. E-Nucl. Phys. **19**, 493 (2010).
[11] P. Jachimowicz, M. Kowal, and J. Skalski, Phys. Rev. C **85**, 034305 (2012).
[12] H, Flocard, P. Quentin, A. K. Kerman, D, Vautherin,. Nucl. Phys. **A203**, 433 (1973).
[13] B. Hayes, Am. Sci. **88**, 481 (2000).
[14] N. Dubray, D. Regnier, Comp. Phys. Comm. **183**, 2035 (2012).
[15] S. G. Nilsson, Kgl. Danske Videnskab. Selskab. Mat.-Fys. Medd. **29**:No. 16 (1955).
[16] S. G. Nilsson, C. F. Tsang, A. Sobiczewski, Z. Szymański, S. Wycech, C. Gustafson, I.-L. Lamm, P. Möller, and B. Nilsson, Nucl. Phys. **A131** (1969) 1.
[17] S. Ćwiok, J. Dudek, W Nazarewicz, J. Skalski, and T. Werner, Comput. Phys. Commun. **46** 379 (1987).
[18] M. Bolsterli, E. O. Fiset, J. R. Nix, and J. L. Norton, Phys. Rev. C **5** (1972) 1050.
[19] H. J. Krappe, J. R. Nix, and A. J. Sierk, Phys. Rev. C **20** (1979) 992.
[20] W. D. Myers and W. J. Swiatecki, Nucl. Phys. **81** (1966) 1.
[21] W. D. Myers and W. J. Swiatecki, Ark. Fys. **36** (1967) 343.
[22] K. T. R. Davies, A. J. Sierk, and J. R. Nix, Phys. Rev. C **13** (1976) 2385.
[23] N. Bohr and J. A. Wheeler, Phys. Rev. **56** (1939) 426.
[24] O. Hahn and F. Strassmann, Naturwiss. **27** (1939) 11.
[25] L. Meitner and O. R. Frisch, Nature **143** (1939) 239.
[26] O. R. Frisch, Nature **143** (1939) 276.
[27] H. A. Bethe and R. F. Bacher, Rev. Mod. Phys. **8** 82 (1936).
[28] P. Möller, J. R. Nix, and W. J. Swiatecki, Nucl. Phys. **A492**, 349 (1989).
[29] W. D. Myers and W. J. Swiatecki, Ann. Phys. (N. Y.) **55** (1969) 395.
[30] P. Möller and J. R. Nix, Proc. Third IAEA Symp. on the physics and chemistry of fission, Rochester, 1973, vol. I (IAEA, Vienna, 1974) p. 103.
[31] P. Möller and J. R. Nix, Nucl. Phys. **A229** (1974) 269.
[32] P. Möller, S. G. Nilsson, and J. R. Nix, Nucl. Phys. **A229** (1974) 292.
[33] P. Möller and J. R. Nix, Nucl. Phys. **A361**, 117 (1981).
[34] P. Möller and J. R. Nix, Nucl. Phys. **A536** (1992) 20.
[35] P. Möller and S. G. Nilsson, Phys. Lett. **31B** (1970) 283.
[36] L. Wilets, Theories of nuclear fission (Clarendon Press, Oxford, 1964).
[37] J. Randrup and P. Möller, Phys. Rev. Lett. **106**, 132503 (2011).
[38] J. Randrup, P. Möller, and A. J. Sierk, Phys. Rev. C **84**, 034613 (2011).
[39] J. Randrup and P. Möller, Phys. Rev. C **88**, 064606 (2013).
[40] J. Blons, R Fabbro, C. Mazur, D. Paya, M. Ribrag, Y. Patin, Nucl. Phys. **A477**, 231 (1988).
[41] T. Ichikawa, P. Möller, and A. J. Sierk, Phys. Rev. C **87**, 054326 (2013).
[42] L. Csige, M. Csatlós, T. Faestermann, Z. Gácsi, J. Gulyás, D. Habs, R. Hertenberger, A. Krasznahorkay, R. Lutter, H. J. Maier. P. G. Thirolf, H.-F. Wirth, Phys. Rev. C **80**, 054306 (2009).
[43] L. Csige, M. Csatlós, T. Faestermann, J. Gulyás, D. Habs, R. Hertenberger, M. Hunyadi, A. Krasznahorkay, H. J. Maier, P. G. Thirolf, H.-F. -Wirth, Phys. Rev. C **85**, 054306 (2012).
[44] L. Csige, D. M. Filipescu, T. Glodariu, J. Gulyás, M. M. Günther, D. Habs, H. J. Karwowski, A. Krasznahorkay, G. C Rich, M. Sin, L. Stroe, O.Tesileunu, and P. G. Thirolf, Phys. Rev. C **87**, 044321 (2013).
[45] A. N. Andreyev M. Huyse, and P. Van Duppen, Rev. Mod. Phys. **85**, 1541 (2013).
[46] M. Veselský, A. N. Andreyev, S.Antalic, M. Huyse, P. Möller, K. Nishio, A. J. Sierk, P. Van Duppen, and M. Venhart, Phys. Rev. C **86**, 024308 (2012).
[47] W. J. Swiatecki, Phys. Rev. **100**, 937 (1955).
[48] Z. Patyk, A. Sobiczewski, P. Armbruster and K.-H. Schmidt, Nucl. Phys. **A491**, 267 (1989).
[49] J. Randrup, C. F. Tsang, P. Möller, S. G. Nilsson, and S. E. Larsson, Nucl. Phys. **A217**, 221 (1973).
[50] J. Randrup, S. E. Larsson, P. Möller, S. G. Nilsson, K. Pomorski, and A. Sobiczewski, Phys. Rev. C **13**, 229 (1976).

[51] A. Baran, K. Pomorski, A. Łukasiak, and A. Sobiczewski, Nucl. Phys. **A361**, 83 (1981).
[52] A. Staszczak, A. Baran, J. Dobaczewski, and W. Nazarewicz, Phys. Rev. C **80**, 014309 (2009).
[53] A. Baran, A. Staszczak, and W. Nazarewicz, Int. J. Mod. Phys. E **20**, 557 (2011).
[54] B. B. Back, O. Hansen, H. C. Britt, and J. D. Garrett, Phys. Rev. C **9** (1974) 1924.
[55] B. B. Back, H. C. Britt, O. Hansen, B. Leroux, and J. D. Garrett, Phys. Rev. C **10** (1974) 1948.
[56] H. C. Britt, Proc. 4th IAEA Symp. on physics and chemistry of fission, Jülich, 1979, vol. I (IAEA, Vienna, 1980) p. 3.
[57] S. Bjørnholm and J. E. Lynn, Rev. Mod. Phys. **52** (1980) 725.
[58] G. Henning1, A. Lopez-Martens , T.L. Khoo, D. Seweryniak, M. Alcorta, M. Asai, B. B. Back, P. Bertone, D. Boilley, M. P. Carpenter, C. J. Chiara, P. Chowdhury, B. Gall, P. T. Greenlees, G. Gurdal, K. Hauschild, A. Heinz, C. R. Hoffman, R. V. F. Janssens, A. V. Karpov, B. P. Kay, F. G. Kondev, S. Lakshmi, T. Lauristen, C. J. Lister, E. A. McCutchan, C. Nair, J. Piot, D. Potterveld, P. Reiter1, N. Rowley, A. M. Rogers, and S. Zhu, EPJ Web of Conferences **66** 02046 (2014).
[59] S. Hofmann, Superheavy Nuclei, in Encyclopedia of Nuclear Physics and its Application, Edited by Reinhard Stock, Wiley-VCH Verlag GmbH & Co., Weinheim, Germany, 2013, pp. 213–246.
[60] W. D. Myers and W. J. Swiatecki, Nucl. Phys. **A612**, 249 (1997).
[61] S. A. Becker, Carnegie Observatories Astrophysics Series, Vol 4, Origin and Evolution of the Elements, 2003, ed. A. McWilliam and M. Rauch (Pasadena: Carnegie Observatories, URL: symposia.obs.carnegiescience.edu/series/symposium4 /ms/becker.ps.gz.
[62] P. Möller, J. R. Nix, and K.-L. Kratz, Atomic Data Nucl. Data Tables **66**, 131 (1997).
[63] N. E. Holden and D. C. Hoffman, Pure and Appl. Chem. **72**, 1525 (2000).
[64] N. E. Holden and D. C. Hoffman, Pure and Appl. Chem. **73**, 1225 (2001).
[65] U. Mosel and H. W. Schmitt, Phys. Rev. C **4**, 2185 (1971).
[66] P. Möller, J. R. Nix, and W. J. Swiatecki, Nucl. Phys. **A469**, 1 (1987).

Calculated Fission-Barrier Heights

N	A	$B_{\rm f}$ (MeV)
$Z = 51$ (Sb)		
120	171	42.48
121	172	43.34
$Z = 52$ (Te)		
119	171	41.24
120	172	41.73
121	173	42.63
122	174	43.12
123	175	43.87
124	176	44.38
$Z = 53$ (I)		
118	171	40.35
119	172	41.42
120	173	41.76
121	174	42.43
122	175	42.68
123	176	43.56
124	177	43.98
125	178	45.53
126	179	45.87
$Z = 54$ (Xe)		
117	171	38.87
118	172	39.50
119	173	40.40
120	174	40.77
121	175	41.43
122	176	41.72
123	177	42.51
124	178	42.94
125	179	44.48
126	180	44.73
127	181	43.46
128	182	42.04
$Z = 55$ (Cs)		
116	171	38.23
117	172	38.95
118	173	39.34

Calculated Fission-Barrier Heights

N	A	$B_{\rm f}$ (MeV)
119	174	40.13
120	175	40.44
121	176	41.34
122	177	41.47
123	178	42.31
124	179	42.71
125	180	44.24
126	181	44.51
127	182	43.33
128	183	42.12
129	184	40.77
130	185	39.26
$Z = 56$ (Ba)		
115	171	36.71
116	172	37.22
117	173	37.85
118	174	38.29
119	175	39.14
120	176	39.32
121	177	40.20
122	178	40.39
123	179	41.29
124	180	41.75
125	181	43.23
126	182	43.36
127	183	42.27
128	184	41.25
129	185	39.85
130	186	38.40
131	187	37.68
132	188	36.74
133	189	36.60
$Z = 57$ (La)		
114	171	35.64
115	172	36.24
116	173	36.81
117	174	37.36
118	175	37.79
119	176	38.61
120	177	39.04
121	178	39.79
122	179	40.18
123	180	41.01
124	181	41.50
125	182	42.90
126	183	43.20
127	184	42.20
128	185	40.94
129	186	39.77
130	187	38.41
131	188	37.79
132	189	36.97
133	190	36.61
134	191	35.39
135	192	34.28
$Z = 58$ (Ce)		
113	171	34.22
114	172	34.49
115	173	35.20
116	174	35.47

Calculated Fission-Barrier Heights

N	A	$B_{\rm f}$ (MeV)
117	175	36.41
118	176	36.76
119	177	37.42
120	178	37.81
121	179	38.62
122	180	39.05
123	181	39.94
124	182	40.59
125	183	41.89
126	184	42.24
127	185	41.23
128	186	40.17
129	187	38.83
130	188	37.53
131	189	36.93
132	190	36.19
133	191	35.72
134	192	35.01
135	193	34.02
136	194	33.09
137	195	32.25
$Z = 59$ (Pr)		
112	171	33.38
113	172	33.74
114	173	33.91
115	174	34.32
116	175	34.61
117	176	35.62
118	177	36.09
119	178	36.76
120	179	37.19
121	180	38.03
122	181	38.50
123	182	39.57
124	183	40.13
125	184	41.47
126	185	41.88
127	186	40.92
128	187	39.73
129	188	38.62
130	189	37.41
131	190	36.98
132	191	36.05
133	192	35.47
134	193	34.50
135	194	34.11
136	195	33.15
137	196	32.54
138	197	31.96
139	198	31.33
$Z = 60$ (Nd)		
111	171	32.65
112	172	32.73
113	173	32.98
114	174	33.24
115	175	33.50
116	176	33.73
117	177	34.54
118	178	35.10
119	179	35.83

Calculated Fission-Barrier Heights

N	A	$B_{\rm f}$ (MeV)
120	180	36.02
121	181	36.89
122	182	37.44
123	183	38.51
124	184	39.11
125	185	40.47
126	186	40.86
127	187	39.83
128	188	38.86
129	189	37.60
130	190	36.51
131	191	35.97
132	192	35.02
133	193	34.46
134	194	33.43
135	195	32.65
136	196	31.85
137	197	32.09
138	198	31.61
139	199	30.94
140	200	30.76
141	201	30.58
$Z = 61$ (Pm)		
110	171	32.33
111	172	32.25
112	173	32.25
113	174	32.54
114	175	32.62
115	176	32.91
116	177	33.10
117	178	33.84
118	179	34.27
119	180	35.04
120	181	35.28
121	182	36.40
122	183	36.83
123	184	37.96
124	185	38.61
125	186	40.01
126	187	40.36
127	188	39.42
128	189	38.44
129	190	37.31
130	191	36.28
131	192	35.87
132	193	34.87
133	194	34.23
134	195	33.15
135	196	32.48
136	197	31.89
137	198	31.82
138	199	31.43
139	200	31.15
140	201	30.91
141	202	30.78
142	203	30.74
143	204	30.85
144	205	30.55
$Z = 62$ (Sm)		
109	171	32.27

Calculated Fission-Barrier Heights

N	A	$B_{\rm f}$ (MeV)
110	172	32.19
111	173	31.96
112	174	32.04
113	175	32.15
114	176	32.07
115	177	32.50
116	178	32.59
117	179	33.13
118	180	33.70
119	181	34.11
120	182	34.47
121	183	35.41
122	184	35.94
123	185	36.97
124	186	37.62
125	187	38.94
126	188	39.36
127	189	38.37
128	190	37.42
129	191	36.23
130	192	35.28
131	193	34.85
132	194	33.81
133	195	33.16
134	196	32.07
135	197	31.44
136	198	31.00
137	199	30.93
138	200	30.66
139	201	30.52
140	202	30.26
141	203	30.29
142	204	30.33
143	205	30.33
144	206	30.23
145	207	29.96
146	208	29.63
$Z = 63$ (Eu)		
108	171	32.51
109	172	32.61
110	173	31.96
111	174	31.87
112	175	31.62
113	176	31.80
114	177	31.67
115	178	31.98
116	179	32.15
117	180	32.66
118	181	33.01
119	182	33.62
120	183	34.06
121	184	34.93
122	185	35.36
123	186	36.33
124	187	36.90
125	188	38.37
126	189	38.73
127	190	37.75
128	191	36.78
129	192	35.84

Calculated Fission-Barrier Heights

N	A	$B_{\rm f}$ (MeV)
130	193	34.82
131	194	34.65
132	195	33.47
133	196	32.85
134	197	31.75
135	198	31.29
136	199	30.83
137	200	30.83
138	201	30.55
139	202	30.50
140	203	30.25
141	204	30.34
142	205	30.37
143	206	30.39
144	207	30.24
145	208	30.04
146	209	29.70
147	210	29.56
148	211	29.37
$Z = 64$ (Gd)		
107	171	32.85
108	172	32.49
109	173	32.33
110	174	31.92
111	175	31.71
112	176	31.47
113	177	31.30
114	178	31.27
115	179	31.72
116	180	31.66
117	181	32.20
118	182	32.59
119	183	33.06
120	184	33.53
121	185	34.13
122	186	34.52
123	187	35.37
124	188	35.91
125	189	37.25
126	190	37.70
127	191	36.64
128	192	35.74
129	193	34.77
130	194	33.84
131	195	33.45
132	196	32.43
133	197	31.80
134	198	30.83
135	199	30.35
136	200	30.00
137	201	29.98
138	202	29.82
139	203	29.61
140	204	29.60
141	205	29.45
142	206	29.60
143	207	29.58
144	208	29.58
145	209	29.50
146	210	29.12

Calculated Fission-Barrier Heights

N	A	$B_{\rm f}$ (MeV)
147	211	29.00
148	212	28.75
149	213	28.85
150	214	28.69
$Z = 65$ (Tb)		
106	171	33.01
107	172	32.80
108	173	32.60
109	174	32.17
110	175	31.84
111	176	31.41
112	177	30.95
113	178	30.99
114	179	30.91
115	180	31.31
116	181	31.43
117	182	31.92
118	183	32.08
119	184	32.51
120	185	32.94
121	186	33.67
122	187	33.93
123	188	34.78
124	189	35.25
125	190	36.39
126	191	36.97
127	192	35.86
128	193	34.90
129	194	34.12
130	195	32.99
131	196	32.72
132	197	31.76
133	198	31.19
134	199	30.32
135	200	29.99
136	201	29.63
137	202	29.83
138	203	29.60
139	204	29.55
140	205	29.49
141	206	29.40
142	207	29.45
143	208	29.60
144	209	29.55
145	210	29.57
146	211	29.16
147	212	29.07
148	213	28.69
149	214	28.98
150	215	28.72
151	216	28.62
152	217	28.31
153	218	27.84
$Z = 66$ (Dy)		
105	171	32.57
106	172	31.84
107	173	32.35
108	174	32.39
109	175	31.98
110	176	31.55

Calculated Fission-Barrier Heights

N	A	$B_{\rm f}$ (MeV)
111	177	31.19
112	178	30.85
113	179	30.65
114	180	30.60
115	181	31.05
116	182	31.01
117	183	31.43
118	184	31.58
119	185	31.99
120	186	32.39
121	187	32.99
122	188	33.15
123	189	33.86
124	190	34.37
125	191	35.51
126	192	36.05
127	193	34.88
128	194	34.06
129	195	33.15
130	196	32.08
131	197	31.55
132	198	30.57
133	199	29.99
134	200	29.22
135	201	28.88
136	202	28.60
137	203	28.79
138	204	28.64
139	205	28.55
140	206	28.46
141	207	28.43
142	208	28.47
143	209	28.65
144	210	28.65
145	211	28.73
146	212	28.54
147	213	28.27
148	214	28.20
149	215	28.21
150	216	28.13
151	217	28.02
152	218	27.62
153	219	27.28
154	220	26.84
155	221	26.53
$Z = 67$ (Ho)		
104	171	31.25
105	172	31.49
106	173	31.15
107	174	31.57
108	175	31.40
109	176	31.71
110	177	31.30
111	178	30.91
112	179	30.42
113	180	30.36
114	181	30.28
115	182	30.61
116	183	30.55
117	184	31.09

Calculated Fission-Barrier Heights

N	A	$B_{\rm f}$ (MeV)
118	185	31.04
119	186	31.43
120	187	31.81
121	188	32.43
122	189	32.56
123	190	33.44
124	191	33.68
125	192	34.82
126	193	35.31
127	194	34.28
128	195	33.32
129	196	32.30
130	197	31.22
131	198	30.66
132	199	29.73
133	200	29.29
134	201	28.56
135	202	28.43
136	203	28.19
137	204	28.44
138	205	28.23
139	206	28.58
140	207	28.41
141	208	28.26
142	209	28.25
143	210	28.47
144	211	28.47
145	212	28.56
146	213	28.43
147	214	28.19
148	215	28.10
149	216	28.10
150	217	28.04
151	218	27.99
152	219	27.53
153	220	27.26
154	221	26.79
155	222	26.52
156	223	26.09
157	224	25.73
$Z = 68$ (Er)		
103	171	32.34
104	172	31.21
105	173	31.27
106	174	31.02
107	175	30.51
108	176	30.37
109	177	30.27
110	178	30.10
111	179	29.80
112	180	29.36
113	181	29.60
114	182	29.88
115	183	29.85
116	184	30.04
117	185	30.28
118	186	30.44
119	187	30.90
120	188	31.35
121	189	31.74

Calculated Fission-Barrier Heights

N	A	B_{f} (MeV)
122	190	31.80
123	191	32.55
124	192	32.98
125	193	34.15
126	194	34.51
127	195	33.46
128	196	32.72
129	197	31.55
130	198	30.32
131	199	29.56
132	200	28.59
133	201	28.07
134	202	27.42
135	203	27.23
136	204	27.05
137	205	27.23
138	206	27.04
139	207	27.31
140	208	27.25
141	209	27.21
142	210	27.24
143	211	27.29
144	212	27.42
145	213	27.50
146	214	27.55
147	215	27.31
148	216	27.19
149	217	27.23
150	218	27.20
151	219	27.08
152	220	26.76
153	221	26.49
154	222	26.14
155	223	26.00
156	224	25.64
157	225	25.34
158	226	24.80
159	227	24.50
$Z = 69$ (Tm)		
102	171	30.81
103	172	31.28
104	173	31.02
105	174	31.35
106	175	31.09
107	176	30.87
108	177	30.40
109	178	30.17
110	179	30.01
111	180	29.54
112	181	29.04
113	182	29.03
114	183	29.02
115	184	29.05
116	185	29.16
117	186	29.34
118	187	29.55
119	188	30.00
120	189	30.75
121	190	31.09
122	191	31.18

Calculated Fission-Barrier Heights

N	A	$B_{\rm f}$ (MeV)
123	192	31.93
124	193	32.45
125	194	33.61
126	195	34.02
127	196	32.84
128	197	32.02
129	198	30.82
130	199	29.50
131	200	28.76
132	201	27.86
133	202	27.41
134	203	26.74
135	204	26.59
136	205	26.35
137	206	26.57
138	207	26.47
139	208	26.78
140	209	26.59
141	210	27.07
142	211	26.98
143	212	27.07
144	213	27.14
145	214	27.19
146	215	27.33
147	216	27.15
148	217	26.96
149	218	27.04
150	219	26.88
151	220	26.84
152	221	26.50
153	222	26.38
154	223	26.05
155	224	25.93
156	225	25.57
157	226	25.41
158	227	24.78
159	228	24.64
160	229	24.19
161	230	24.02
$Z = 70$ (Yb)		
101	171	28.60
102	172	29.20
103	173	29.89
104	174	29.84
105	175	30.22
106	176	30.19
107	177	30.47
108	178	30.35
109	179	30.07
110	180	29.82
111	181	29.45
112	182	28.91
113	183	28.54
114	184	28.44
115	185	28.48
116	186	28.34
117	187	28.55
118	188	28.71
119	189	29.08
120	190	29.91

Calculated Fission-Barrier Heights

N	A	$B_{\rm f}$ (MeV)
121	191	30.48
122	192	30.70
123	193	31.42
124	194	31.94
125	195	32.93
126	196	33.36
127	197	32.30
128	198	31.37
129	199	29.98
130	200	28.77
131	201	27.70
132	202	26.78
133	203	26.22
134	204	25.69
135	205	25.39
136	206	25.16
137	207	25.26
138	208	25.20
139	209	25.55
140	210	25.29
141	211	25.67
142	212	25.67
143	213	25.77
144	214	25.88
145	215	25.93
146	216	26.08
147	217	26.04
148	218	25.86
149	219	26.04
150	220	25.87
151	221	25.89
152	222	25.68
153	223	25.53
154	224	25.32
155	225	25.19
156	226	24.80
157	227	24.64
158	228	24.12
159	229	24.02
160	230	23.66
161	231	23.58
162	232	23.32
163	233	23.07
164	234	22.38
$Z = 71$ (Lu)		
100	171	26.54
101	172	27.28
102	173	27.65
103	174	28.42
104	175	28.92
105	176	29.42
106	177	29.54
107	178	29.86
108	179	29.92
109	180	29.89
110	181	29.50
111	182	29.25
112	183	28.62
113	184	28.23
114	185	28.00

Calculated Fission-Barrier Heights

N	A	$B_{\rm f}$ (MeV)
115	186	27.90
116	187	27.68
117	188	28.00
118	189	28.26
119	190	28.44
120	191	29.43
121	192	29.91
122	193	30.09
123	194	30.82
124	195	31.26
125	196	32.25
126	197	32.57
127	198	31.67
128	199	30.75
129	200	29.36
130	201	28.10
131	202	26.98
132	203	26.05
133	204	25.53
134	205	24.99
135	206	24.73
136	207	24.36
137	208	24.53
138	209	24.35
139	210	24.62
140	211	24.58
141	212	25.11
142	213	25.05
143	214	25.44
144	215	25.46
145	216	25.63
146	217	25.63
147	218	25.69
148	219	25.51
149	220	25.68
150	221	25.50
151	222	25.63
152	223	25.49
153	224	25.35
154	225	25.09
155	226	25.03
156	227	24.59
157	228	24.50
158	229	23.95
159	230	23.94
160	231	23.60
161	232	23.60
162	233	23.37
163	234	23.18
164	235	22.44
165	236	22.02
166	237	21.35
$Z = 72$ (Hf)		
99	171	24.26
100	172	24.65
101	173	25.30
102	174	25.84
103	175	26.52
104	176	27.09
105	177	27.59

Calculated Fission-Barrier Heights

N	A	B_{f} (MeV)
106	178	28.21
107	179	28.92
108	180	28.72
109	181	28.93
110	182	28.65
111	183	28.75
112	184	28.07
113	185	27.64
114	186	27.24
115	187	26.98
116	188	26.90
117	189	27.01
118	190	27.44
119	191	27.71
120	192	28.61
121	193	29.30
122	194	29.61
123	195	30.32
124	196	30.80
125	197	31.65
126	198	32.03
127	199	31.12
128	200	30.19
129	201	28.93
130	202	27.70
131	203	26.17
132	204	25.03
133	205	24.44
134	206	23.93
135	207	23.53
136	208	23.12
137	209	23.08
138	210	22.90
139	211	23.31
140	212	23.25
141	213	23.71
142	214	23.71
143	215	24.22
144	216	24.07
145	217	24.25
146	218	24.23
147	219	24.43
148	220	24.29
149	221	24.49
150	222	24.41
151	223	24.46
152	224	24.44
153	225	24.30
154	226	24.11
155	227	24.08
156	228	23.65
157	229	23.56
158	230	23.18
159	231	23.09
160	232	22.83
161	233	22.81
162	234	22.66
163	235	22.39
164	236	22.03
165	237	21.57

Calculated Fission-Barrier Heights

N	A	$B_{\rm f}$ (MeV)
166	238	20.94
167	239	20.74
168	240	20.04
$Z = 73$ (Ta)		
98	171	21.96
99	172	22.76
100	173	23.14
101	174	23.93
102	175	24.41
103	176	25.17
104	177	25.42
105	178	26.20
106	179	26.62
107	180	27.26
108	181	27.37
109	182	27.58
110	183	27.62
111	184	28.00
112	185	27.79
113	186	27.72
114	187	27.14
115	188	26.84
116	189	26.66
117	190	26.91
118	191	27.09
119	192	27.48
120	193	27.79
121	194	28.70
122	195	29.03
123	196	29.80
124	197	30.19
125	198	31.07
126	199	31.35
127	200	30.55
128	201	29.64
129	202	28.48
130	203	27.06
131	204	25.86
132	205	24.55
133	206	23.91
134	207	23.28
135	208	23.13
136	209	22.60
137	210	22.75
138	211	22.70
139	212	22.51
140	213	22.78
141	214	23.19
142	215	23.24
143	216	23.69
144	217	23.46
145	218	23.65
146	219	23.71
147	220	23.92
148	221	23.78
149	222	23.90
150	223	23.90
151	224	24.02
152	225	23.98
153	226	23.94

Calculated Fission-Barrier Heights

N	A	B_{f} (MeV)
154	227	23.69
155	228	23.64
156	229	23.26
157	230	23.20
158	231	22.75
159	232	22.83
160	233	22.53
161	234	22.59
162	235	22.46
163	236	22.27
164	237	21.91
165	238	21.55
166	239	20.94
167	240	20.77
168	241	20.12
169	242	19.95
170	243	19.48
$Z = 74$ (W)		
97	171	19.82
98	172	20.03
99	173	20.71
100	174	21.16
101	175	21.80
102	176	22.25
103	177	22.97
104	178	23.47
105	179	24.14
106	180	24.57
107	181	25.13
108	182	25.26
109	183	25.58
110	184	25.44
111	185	25.71
112	186	25.85
113	187	26.36
114	188	26.71
115	189	26.40
116	190	26.43
117	191	26.55
118	192	26.86
119	193	27.01
120	194	27.44
121	195	27.99
122	196	28.45
123	197	29.18
124	198	29.63
125	199	30.69
126	200	30.96
127	201	30.05
128	202	29.28
129	203	28.08
130	204	26.83
131	205	25.26
132	206	24.09
133	207	23.14
134	208	22.79
135	209	22.42
136	210	21.83
137	211	21.95
138	212	21.77

Calculated Fission-Barrier Heights

N	A	$B_{\rm f}$ (MeV)
139	213	21.83
140	214	21.61
141	215	22.07
142	216	22.08
143	217	22.49
144	218	22.27
145	219	22.16
146	220	22.40
147	221	22.46
148	222	22.44
149	223	22.53
150	224	22.64
151	225	22.68
152	226	22.71
153	227	22.66
154	228	22.45
155	229	22.47
156	230	22.08
157	231	21.99
158	232	21.60
159	233	21.69
160	234	21.49
161	235	21.49
162	236	21.49
163	237	21.27
164	238	20.96
165	239	20.80
166	240	20.27
167	241	20.19
168	242	19.66
169	243	19.56
170	244	19.17
171	245	19.23
172	246	18.74
173	247	18.59
$Z = 75$ (Re)		
96	171	17.51
97	172	17.94
98	173	18.13
99	174	18.81
100	175	19.23
101	176	19.95
102	177	20.56
103	178	21.38
104	179	21.82
105	180	22.50
106	181	22.91
107	182	23.49
108	183	23.62
109	184	23.77
110	185	23.66
111	186	24.13
112	187	24.12
113	188	24.77
114	189	25.13
115	190	25.99
116	191	26.24
117	192	26.37
118	193	26.57
119	194	26.64

Calculated Fission-Barrier Heights

N	A	$B_{\rm f}$ (MeV)
120	195	26.76
121	196	27.44
122	197	27.93
123	198	28.69
124	199	29.07
125	200	29.91
126	201	30.22
127	202	29.48
128	203	28.54
129	204	27.39
130	205	26.18
131	206	25.13
132	207	23.73
133	208	22.96
134	209	22.37
135	210	22.22
136	211	21.72
137	212	21.67
138	213	21.62
139	214	21.68
140	215	21.18
141	216	21.37
142	217	21.09
143	218	21.36
144	219	21.33
145	220	21.43
146	221	21.74
147	222	21.91
148	223	22.00
149	224	22.00
150	225	22.06
151	226	22.09
152	227	22.11
153	228	22.13
154	229	21.68
155	230	21.65
156	231	21.35
157	232	21.47
158	233	21.12
159	234	21.24
160	235	20.93
161	236	21.05
162	237	21.02
163	238	20.94
164	239	20.62
165	240	20.44
166	241	19.98
167	242	19.94
168	243	19.41
169	244	19.42
170	245	19.12
171	246	19.28
172	247	18.75
173	248	18.68
174	249	18.16
175	250	17.93
$Z = 76$ (Os)		
95	171	15.38
96	172	15.49
97	173	15.87

Calculated Fission-Barrier Heights

N	A	B_{f} (MeV)
98	174	16.01
99	175	16.37
100	176	16.97
101	177	17.58
102	178	18.12
103	179	18.79
104	180	19.49
105	181	20.17
106	182	20.76
107	183	21.20
108	184	21.29
109	185	21.41
110	186	21.44
111	187	21.67
112	188	21.75
113	189	22.38
114	190	22.89
115	191	23.85
116	192	24.84
117	193	25.33
118	194	25.58
119	195	25.84
120	196	26.15
121	197	26.75
122	198	27.29
123	199	28.07
124	200	28.54
125	201	29.55
126	202	29.83
127	203	29.07
128	204	28.21
129	205	27.08
130	206	25.98
131	207	24.67
132	208	23.29
133	209	22.24
134	210	21.74
135	211	21.53
136	212	21.04
137	213	20.80
138	214	20.46
139	215	20.41
140	216	20.12
141	217	19.75
142	218	19.50
143	219	19.57
144	220	19.57
145	221	19.84
146	222	19.90
147	223	20.25
148	224	20.41
149	225	20.50
150	226	20.66
151	227	20.67
152	228	20.66
153	229	20.39
154	230	19.94
155	231	19.94
156	232	19.79
157	233	20.14

Calculated Fission-Barrier Heights

N	A	B_{f} (MeV)
158	234	19.80
159	235	19.70
160	236	19.62
161	237	19.79
162	238	19.97
163	239	19.78
164	240	19.21
165	241	19.22
166	242	18.75
167	243	18.78
168	244	18.53
169	245	18.61
170	246	18.47
171	247	18.68
172	248	18.28
173	249	18.17
174	250	17.78
175	251	17.26
176	252	17.37
177	253	18.11
$Z = 77$ (Ir)		
94	171	13.83
95	172	14.18
96	173	13.98
97	174	14.11
98	175	14.14
99	176	14.66
100	177	14.77
101	178	15.47
102	179	16.03
103	180	16.65
104	181	17.26
105	182	17.82
106	183	18.30
107	184	18.84
108	185	18.98
109	186	19.53
110	187	19.59
111	188	20.06
112	189	20.15
113	190	20.69
114	191	20.94
115	192	22.19
116	193	23.18
117	194	23.84
118	195	24.31
119	196	24.95
120	197	25.27
121	198	26.22
122	199	26.92
123	200	27.70
124	201	28.18
125	202	29.05
126	203	29.35
127	204	28.46
128	205	27.77
129	206	26.69
130	207	25.59
131	208	24.27
132	209	22.95

Calculated Fission-Barrier Heights

N	A	$B_{\rm f}$ (MeV)
133	210	21.98
134	211	21.45
135	212	21.13
136	213	20.75
137	214	20.50
138	215	19.99
139	216	19.49
140	217	18.91
141	218	18.58
142	219	18.31
143	220	18.46
144	221	18.27
145	222	18.57
146	223	18.62
147	224	18.99
148	225	19.08
149	226	19.48
150	227	19.49
151	228	19.83
152	229	19.46
153	230	19.44
154	231	18.76
155	232	18.97
156	233	18.88
157	234	19.17
158	235	18.79
159	236	18.67
160	237	18.67
161	238	18.93
162	239	19.09
163	240	18.93
164	241	18.49
165	242	18.42
166	243	17.94
167	244	18.12
168	245	18.04
169	246	18.16
170	247	17.94
171	248	18.50
172	249	18.17
173	250	18.03
174	251	17.57
175	252	17.73
176	253	17.45
177	254	18.25
178	255	18.03
179	256	18.17
$Z = 78$ (Pt)		
93	171	11.36
94	172	11.73
95	173	12.23
96	174	12.39
97	175	12.52
98	176	12.38
99	177	12.48
100	178	12.82
101	179	13.34
102	180	13.78
103	181	14.43
104	182	14.90

Calculated Fission-Barrier Heights

N	A	B_{f} (MeV)
105	183	15.46
106	184	16.09
107	185	16.66
108	186	17.06
109	187	17.59
110	188	17.75
111	189	18.26
112	190	18.80
113	191	19.60
114	192	20.08
115	193	20.84
116	194	21.47
117	195	22.26
118	196	23.01
119	197	23.67
120	198	24.54
121	199	25.52
122	200	26.30
123	201	27.06
124	202	27.51
125	203	28.34
126	204	28.50
127	205	27.64
128	206	26.98
129	207	25.77
130	208	24.77
131	209	23.44
132	210	22.33
133	211	21.48
134	212	20.81
135	213	20.32
136	214	19.74
137	215	19.44
138	216	18.97
139	217	18.35
140	218	17.75
141	219	17.32
142	220	16.90
143	221	16.70
144	222	16.67
145	223	16.70
146	224	16.78
147	225	16.98
148	226	17.08
149	227	17.55
150	228	17.45
151	229	17.75
152	230	17.65
153	231	17.33
154	232	17.22
155	233	17.47
156	234	17.42
157	235	17.54
158	236	17.24
159	237	17.18
160	238	17.33
161	239	17.49
162	240	17.63
163	241	17.56
164	242	17.18

Calculated Fission-Barrier Heights

N	A	$B_{\rm f}$ (MeV)
165	243	16.97
166	244	16.82
167	245	16.80
168	246	16.70
169	247	17.00
170	248	16.86
171	249	17.30
172	250	17.33
173	251	17.54
174	252	17.33
175	253	17.54
176	254	17.49
177	255	17.77
178	256	17.75
179	257	17.89
180	258	17.65
181	259	17.70
182	260	17.33
$Z = 79$ (Au)		
92	171	10.83
93	172	10.94
94	173	10.94
95	174	10.64
96	175	11.00
97	176	11.28
98	177	11.07
99	178	11.23
100	179	11.36
101	180	11.83
102	181	12.28
103	182	12.76
104	183	13.20
105	184	13.84
106	185	14.31
107	186	15.03
108	187	15.33
109	188	16.01
110	189	16.57
111	190	17.16
112	191	17.99
113	192	18.87
114	193	19.26
115	194	19.96
116	195	20.54
117	196	21.47
118	197	22.31
119	198	23.16
120	199	23.97
121	200	25.07
122	201	25.78
123	202	26.53
124	203	27.01
125	204	27.95
126	205	28.03
127	206	27.09
128	207	26.36
129	208	25.36
130	209	24.25
131	210	22.93
132	211	21.87

Calculated Fission-Barrier Heights

N	A	$B_{\rm f}$ (MeV)
133	212	21.29
134	213	20.54
135	214	19.95
136	215	19.25
137	216	18.84
138	217	18.24
139	218	17.77
140	219	16.95
141	220	16.41
142	221	15.77
143	222	15.58
144	223	15.51
145	224	15.44
146	225	15.35
147	226	15.71
148	227	15.79
149	228	16.52
150	229	16.18
151	230	16.98
152	231	16.31
153	232	16.48
154	233	16.25
155	234	16.50
156	235	16.36
157	236	16.46
158	237	16.23
159	238	16.41
160	239	16.47
161	240	16.58
162	241	16.63
163	242	16.61
164	243	16.24
165	244	16.08
166	245	15.69
167	246	15.99
168	247	16.24
169	248	16.77
170	249	16.94
171	250	17.57
172	251	17.57
173	252	17.82
174	253	17.39
175	254	17.70
176	255	17.77
177	256	17.64
178	257	17.61
179	258	17.86
180	259	17.60
181	260	17.61
182	261	17.31
183	262	17.32
184	263	17.27
$Z = 80$ (Hg)		
91	171	10.03
92	172	9.81
93	173	9.79
94	174	9.63
95	175	9.77
96	176	9.62
97	177	9.41

Calculated Fission-Barrier Heights

N	A	B_{f} (MeV)
98	178	9.32
99	179	9.68
100	180	9.81
101	181	10.27
102	182	10.85
103	183	11.32
104	184	11.92
105	185	12.43
106	186	12.99
107	187	13.50
108	188	13.98
109	189	14.52
110	190	15.22
111	191	16.02
112	192	16.75
113	193	17.56
114	194	18.10
115	195	18.79
116	196	19.65
117	197	20.48
118	198	21.45
119	199	22.24
120	200	23.23
121	201	24.05
122	202	24.79
123	203	25.55
124	204	26.11
125	205	27.09
126	206	27.21
127	207	26.10
128	208	25.51
129	209	24.37
130	210	23.32
131	211	22.17
132	212	21.27
133	213	20.44
134	214	19.80
135	215	19.00
136	216	18.33
137	217	17.73
138	218	17.04
139	219	16.53
140	220	15.69
141	221	15.13
142	222	14.56
143	223	14.41
144	224	14.13
145	225	14.19
146	226	14.30
147	227	14.59
148	228	14.71
149	229	15.09
150	230	14.95
151	231	15.16
152	232	14.97
153	233	15.11
154	234	14.85
155	235	15.09
156	236	14.97
157	237	14.99

Calculated Fission-Barrier Heights

N	A	B_{f} (MeV)
158	238	14.91
159	239	14.90
160	240	14.97
161	241	15.21
162	242	15.24
163	243	15.22
164	244	14.90
165	245	14.71
166	246	15.11
167	247	15.50
168	248	15.77
169	249	16.12
170	250	16.40
171	251	16.79
172	252	16.89
173	253	17.28
174	254	17.38
175	255	17.74
176	256	17.62
177	257	17.77
178	258	17.76
179	259	18.02
180	260	17.79
181	261	17.84
182	262	17.69
183	263	17.75
184	264	17.41
185	265	16.52
186	266	15.63
$Z = 81$ (Tl)		
92	173	9.11
93	174	8.96
94	175	9.13
95	176	9.19
96	177	9.04
97	178	9.01
98	179	8.81
99	180	8.65
100	181	8.86
101	182	8.98
102	183	9.49
103	184	9.87
104	185	10.44
105	186	10.97
106	187	11.48
107	188	12.11
108	189	12.74
109	190	13.49
110	191	14.31
111	192	15.13
112	193	15.99
113	194	16.38
114	195	17.08
115	196	18.04
116	197	18.85
117	198	19.73
118	199	20.63
119	200	21.66
120	201	22.23
121	202	23.29

Calculated Fission-Barrier Heights

N	A	B_{f} (MeV)
122	203	24.04
123	204	24.80
124	205	25.49
125	206	26.38
126	207	26.50
127	208	25.55
128	209	24.72
129	210	23.55
130	211	22.42
131	212	21.58
132	213	20.79
133	214	19.97
134	215	19.19
135	216	18.50
136	217	17.78
137	218	17.31
138	219	16.50
139	220	15.88
140	221	14.99
141	222	14.33
142	223	13.64
143	224	13.49
144	225	13.33
145	226	13.54
146	227	13.53
147	228	13.89
148	229	13.86
149	230	14.15
150	231	13.99
151	232	14.20
152	233	13.96
153	234	14.09
154	235	13.81
155	236	13.94
156	237	13.78
157	238	14.12
158	239	14.02
159	240	14.29
160	241	14.07
161	242	14.31
162	243	14.37
163	244	14.43
164	245	14.19
165	246	14.35
166	247	14.53
167	248	14.88
168	249	15.23
169	250	15.62
170	251	15.98
171	252	16.53
172	253	16.75
173	254	17.20
174	255	17.10
175	256	17.50
176	257	17.58
177	258	17.76
178	259	17.90
179	260	18.33
180	261	18.18
181	262	18.51

Calculated Fission-Barrier Heights

N	A	$B_{\rm f}$ (MeV)
182	263	18.25
183	264	18.37
184	265	17.79
185	266	16.95
186	267	15.93
187	268	14.45
188	269	13.28
$Z = 82$ (Pb)		
93	175	7.62
94	176	7.58
95	177	7.74
96	178	7.99
97	179	8.15
98	180	8.47
99	181	8.48
100	182	8.62
101	183	8.65
102	184	8.92
103	185	9.12
104	186	9.61
105	187	9.83
106	188	10.32
107	189	10.63
108	190	11.18
109	191	11.68
110	192	12.85
111	193	13.57
112	194	14.50
113	195	14.77
114	196	15.66
115	197	16.36
116	198	17.28
117	199	18.09
118	200	18.89
119	201	19.67
120	202	20.48
121	203	20.91
122	204	21.91
123	205	23.08
124	206	23.94
125	207	24.76
126	208	24.95
127	209	23.97
128	210	22.91
129	211	21.88
130	212	20.77
131	213	19.87
132	214	19.13
133	215	18.43
134	216	17.95
135	217	17.48
136	218	16.83
137	219	16.13
138	220	15.33
139	221	14.45
140	222	13.70
141	223	12.89
142	224	12.48
143	225	12.43
144	226	12.34

Calculated Fission-Barrier Heights

N	A	$B_{\rm f}$ (MeV)
145	227	12.30
146	228	12.16
147	229	12.39
148	230	12.58
149	231	12.82
150	232	12.67
151	233	12.90
152	234	12.64
153	235	12.70
154	236	12.41
155	237	12.40
156	238	12.23
157	239	12.37
158	240	12.42
159	241	12.81
160	242	12.77
161	243	13.01
162	244	13.07
163	245	13.21
164	246	13.24
165	247	13.42
166	248	13.60
167	249	13.85
168	250	14.06
169	251	14.61
170	252	14.85
171	253	15.29
172	254	15.28
173	255	15.72
174	256	15.67
175	257	16.18
176	258	16.30
177	259	17.03
178	260	17.33
179	261	17.87
180	262	17.97
181	263	18.30
182	264	18.08
183	265	18.20
184	266	17.71
185	267	16.50
186	268	15.43
187	269	13.94
188	270	12.96
189	271	12.57
190	272	12.09
191	273	11.96
$Z = 83$ (Bi)		
95	178	5.33
96	179	5.40
97	180	5.69
98	181	5.73
99	182	6.40
100	183	6.53
101	184	7.16
102	185	7.38
103	186	7.75
104	187	7.75
105	188	8.14
106	189	8.60

Calculated Fission-Barrier Heights

N	A	B_{f} (MeV)
107	190	9.15
108	191	9.45
109	192	9.99
110	193	10.59
111	194	11.14
112	195	11.79
113	196	12.31
114	197	13.29
115	198	14.23
116	199	15.22
117	200	16.18
118	201	16.99
119	202	17.90
120	203	18.71
121	204	19.59
122	205	20.47
123	206	21.42
124	207	22.28
125	208	23.23
126	209	23.88
127	210	22.74
128	211	21.76
129	212	20.49
130	213	19.17
131	214	17.89
132	215	16.79
133	216	16.05
134	217	15.65
135	218	15.16
136	219	14.45
137	220	14.02
138	221	13.33
139	222	12.58
140	223	12.26
141	224	12.31
142	225	12.14
143	226	11.92
144	227	11.79
145	228	11.71
146	229	11.66
147	230	11.77
148	231	11.44
149	232	11.84
150	233	11.65
151	234	11.87
152	235	11.56
153	236	11.56
154	237	11.36
155	238	11.14
156	239	10.96
157	240	11.28
158	241	11.29
159	242	11.55
160	243	11.44
161	244	11.68
162	245	11.72
163	246	12.08
164	247	11.97
165	248	12.66
166	249	12.78

Calculated Fission-Barrier Heights

N	A	$B_{\rm f}$ (MeV)
167	250	13.10
168	251	13.46
169	252	14.06
170	253	14.25
171	254	14.59
172	255	14.74
173	256	14.94
174	257	14.81
175	258	15.42
176	259	15.81
177	260	16.27
178	261	16.42
179	262	17.06
180	263	17.19
181	264	17.59
182	265	17.41
183	266	17.52
184	267	16.96
185	268	15.81
186	269	14.74
187	270	13.30
188	271	11.66
189	272	11.88
190	273	11.25
191	274	11.23
192	275	10.76
193	276	9.86
$Z = 84$ (Po)		
97	181	3.89
98	182	4.35
99	183	4.89
100	184	5.49
101	185	5.93
102	186	6.35
103	187	6.64
104	188	6.92
105	189	7.27
106	190	7.55
107	191	7.89
108	192	8.25
109	193	8.66
110	194	9.46
111	195	9.59
112	196	10.29
113	197	10.66
114	198	11.52
115	199	12.37
116	200	13.31
117	201	14.18
118	202	15.14
119	203	16.15
120	204	17.02
121	205	18.08
122	206	19.02
123	207	20.01
124	208	20.81
125	209	22.24
126	210	22.14
127	211	21.33
128	212	20.27

Calculated Fission-Barrier Heights

N	A	B_{f} (MeV)
129	213	18.99
130	214	17.76
131	215	16.47
132	216	15.42
133	217	14.56
134	218	13.85
135	219	12.93
136	220	12.47
137	221	12.31
138	222	11.91
139	223	11.70
140	224	11.46
141	225	11.24
142	226	10.98
143	227	10.92
144	228	10.68
145	229	10.66
146	230	10.63
147	231	10.75
148	232	10.69
149	233	10.97
150	234	10.76
151	235	11.08
152	236	10.83
153	237	10.85
154	238	10.49
155	239	10.49
156	240	10.11
157	241	10.28
158	242	10.34
159	243	10.62
160	244	10.61
161	245	10.99
162	246	10.95
163	247	11.42
164	248	11.35
165	249	11.56
166	250	11.69
167	251	12.04
168	252	12.29
169	253	12.83
170	254	12.98
171	255	13.35
172	256	13.73
173	257	13.69
174	258	13.70
175	259	14.20
176	260	14.61
177	261	15.12
178	262	15.24
179	263	15.83
180	264	16.02
181	265	16.41
182	266	16.33
183	267	16.51
184	268	16.05
185	269	14.82
186	270	13.86
187	271	12.36
188	272	11.82

Calculated Fission-Barrier Heights

N	A	B_{f} (MeV)
189	273	11.49
190	274	10.85
191	275	10.84
192	276	10.02
193	277	9.16
194	278	8.48
195	279	7.86
$Z = 85$ (At)		
99	184	4.12
100	185	4.39
101	186	4.68
102	187	5.00
103	188	5.44
104	189	5.56
105	190	5.94
106	191	6.02
107	192	6.76
108	193	7.24
109	194	7.67
110	195	7.96
111	196	8.33
112	197	8.63
113	198	9.10
114	199	9.95
115	200	10.80
116	201	11.73
117	202	12.66
118	203	13.70
119	204	14.72
120	205	15.41
121	206	16.63
122	207	17.46
123	208	18.31
124	209	19.10
125	210	19.99
126	211	20.27
127	212	19.37
128	213	18.56
129	214	17.35
130	215	16.03
131	216	14.99
132	217	14.16
133	218	13.31
134	219	12.46
135	220	12.12
136	221	11.75
137	222	11.64
138	223	11.13
139	224	11.03
140	225	10.74
141	226	10.42
142	227	10.11
143	228	10.02
144	229	9.83
145	230	9.86
146	231	9.78
147	232	9.97
148	233	9.93
149	234	10.18
150	235	10.36

Calculated Fission-Barrier Heights

N	A	B_{f} (MeV)
151	236	10.60
152	237	10.53
153	238	10.31
154	239	10.04
155	240	9.79
156	241	9.58
157	242	9.94
158	243	9.73
159	244	10.19
160	245	10.17
161	246	10.41
162	247	10.42
163	248	10.60
164	249	10.49
165	250	10.75
166	251	10.88
167	252	11.26
168	253	11.47
169	254	12.04
170	255	12.22
171	256	12.53
172	257	13.04
173	258	12.82
174	259	12.94
175	260	13.24
176	261	13.65
177	262	14.18
178	263	14.37
179	264	14.66
180	265	14.81
181	266	15.21
182	267	15.13
183	268	15.30
184	269	14.82
185	270	13.70
186	271	12.88
187	272	11.34
188	273	10.89
189	274	10.46
190	275	10.14
191	276	10.05
192	277	9.12
193	278	8.69
194	279	7.97
195	280	7.13
196	281	6.46
197	282	6.20
$Z = 86$ (Rn)		
100	186	4.19
101	187	4.43
102	188	4.45
103	189	4.62
104	190	4.54
105	191	4.49
106	192	4.63
107	193	5.02
108	194	5.43
109	195	6.05
110	196	6.41
111	197	6.83

Calculated Fission-Barrier Heights

N	A	B_{f} (MeV)
112	198	7.40
113	199	8.09
114	200	8.61
115	201	9.39
116	202	10.29
117	203	11.16
118	204	12.10
119	205	13.20
120	206	14.20
121	207	15.14
122	208	15.94
123	209	16.75
124	210	17.61
125	211	18.47
126	212	18.63
127	213	17.65
128	214	16.69
129	215	15.45
130	216	14.24
131	217	13.52
132	218	12.83
133	219	12.02
134	220	11.47
135	221	11.18
136	222	10.82
137	223	10.57
138	224	10.30
139	225	9.72
140	226	9.45
141	227	9.26
142	228	9.04
143	229	8.88
144	230	8.81
145	231	8.81
146	232	8.82
147	233	8.87
148	234	8.92
149	235	9.21
150	236	9.38
151	237	9.76
152	238	9.70
153	239	9.73
154	240	9.30
155	241	9.17
156	242	8.98
157	243	9.26
158	244	9.12
159	245	9.01
160	246	9.02
161	247	9.28
162	248	9.34
163	249	9.51
164	250	9.40
165	251	9.41
166	252	9.52
167	253	9.81
168	254	10.03
169	255	10.52
170	256	10.81
171	257	11.22

Calculated Fission-Barrier Heights

N	A	B_{f} (MeV)
172	258	11.60
173	259	11.32
174	260	11.35
175	261	11.91
176	262	12.30
177	263	12.79
178	264	12.99
179	265	13.42
180	266	13.55
181	267	13.74
182	268	13.81
183	269	14.07
184	270	13.59
185	271	12.54
186	272	11.68
187	273	10.71
188	274	10.02
189	275	9.74
190	276	9.42
191	277	9.22
192	278	8.45
193	279	8.04
194	280	7.37
195	281	6.62
196	282	6.09
197	283	5.45
198	284	5.13
199	285	4.43
200	286	4.00
$Z = 87$ (Fr)		
102	189	4.24
103	190	4.44
104	191	4.33
105	192	4.43
106	193	4.38
107	194	4.35
108	195	4.48
109	196	4.58
110	197	5.18
111	198	5.82
112	199	6.39
113	200	7.10
114	201	7.62
115	202	8.33
116	203	8.92
117	204	9.64
118	205	10.94
119	206	11.98
120	207	12.85
121	208	13.71
122	209	14.60
123	210	15.40
124	211	16.02
125	212	16.72
126	213	16.66
127	214	15.65
128	215	14.81
129	216	13.46
130	217	12.74
131	218	12.40

Calculated Fission-Barrier Heights

N	A	B_{f} (MeV)
132	219	11.57
133	220	11.33
134	221	10.81
135	222	10.47
136	223	10.02
137	224	9.64
138	225	9.22
139	226	9.02
140	227	8.61
141	228	8.36
142	229	8.12
143	230	8.04
144	231	7.96
145	232	8.01
146	233	7.92
147	234	8.09
148	235	8.15
149	236	8.50
150	237	8.71
151	238	8.96
152	239	9.03
153	240	9.07
154	241	8.83
155	242	8.66
156	243	8.44
157	244	8.45
158	245	8.24
159	246	8.09
160	247	8.12
161	248	8.42
162	249	8.44
163	250	8.66
164	251	8.59
165	252	8.53
166	253	8.53
167	254	8.83
168	255	9.00
169	256	9.56
170	257	9.79
171	258	10.05
172	259	10.40
173	260	10.44
174	261	10.20
175	262	10.95
176	263	11.42
177	264	11.72
178	265	11.91
179	266	12.35
180	267	12.32
181	268	12.65
182	269	12.79
183	270	13.05
184	271	12.54
185	272	11.55
186	273	10.76
187	274	9.74
188	275	9.09
189	276	9.18
190	277	8.93
191	278	8.72

Calculated Fission-Barrier Heights

N	A	$B_{\rm f}$ (MeV)
192	279	8.17
193	280	7.72
194	281	7.03
195	282	6.58
196	283	6.14
197	284	5.60
198	285	5.05
199	286	4.53
200	287	4.01
201	288	3.85
202	289	3.27
$Z = 88$ (Ra)		
104	192	3.92
105	193	3.77
106	194	3.76
107	195	3.46
108	196	3.72
109	197	4.12
110	198	3.99
111	199	4.63
112	200	5.12
113	201	5.85
114	202	6.26
115	203	6.89
116	204	7.49
117	205	8.51
118	206	9.75
119	207	10.82
120	208	11.70
121	209	12.54
122	210	13.26
123	211	14.00
124	212	14.40
125	213	15.11
126	214	14.94
127	215	13.93
128	216	13.01
129	217	11.80
130	218	11.25
131	219	10.81
132	220	10.25
133	221	10.03
134	222	9.57
135	223	9.20
136	224	8.78
137	225	8.40
138	226	8.23
139	227	8.02
140	228	7.61
141	229	7.31
142	230	7.04
143	231	7.01
144	232	6.94
145	233	6.97
146	234	6.90
147	235	7.16
148	236	7.33
149	237	7.70
150	238	7.79
151	239	8.26

Calculated Fission-Barrier Heights

N	A	B_{f} (MeV)
152	240	8.24
153	241	8.24
154	242	7.95
155	243	7.78
156	244	7.49
157	245	7.61
158	246	7.34
159	247	7.39
160	248	7.20
161	249	7.29
162	250	7.21
163	251	7.26
164	252	7.08
165	253	7.14
166	254	7.10
167	255	7.33
168	256	7.48
169	257	7.75
170	258	8.07
171	259	8.52
172	260	9.00
173	261	8.87
174	262	9.03
175	263	9.73
176	264	10.16
177	265	10.73
178	266	10.80
179	267	11.18
180	268	11.15
181	269	11.68
182	270	11.74
183	271	12.02
184	272	11.58
185	273	10.53
186	274	9.78
187	275	8.88
188	276	8.33
189	277	8.48
190	278	8.22
191	279	8.20
192	280	7.64
193	281	7.16
194	282	6.46
195	283	6.10
196	284	5.56
197	285	5.19
198	286	4.77
199	287	4.26
200	288	3.78
201	289	3.39
202	290	2.91
203	291	2.63
204	292	2.24
$Z = 89$ (Ac)		
106	195	3.40
107	196	3.29
108	197	3.24
109	198	3.44
110	199	3.45
111	200	3.64

Calculated Fission-Barrier Heights

N	A	B_{f} (MeV)
112	201	4.05
113	202	4.81
114	203	5.19
115	204	5.72
116	205	6.49
117	206	7.42
118	207	8.46
119	208	9.50
120	209	10.58
121	210	11.31
122	211	12.03
123	212	12.65
124	213	12.99
125	214	13.52
126	215	13.36
127	216	12.19
128	217	11.08
129	218	10.40
130	219	10.03
131	220	9.71
132	221	9.34
133	222	9.13
134	223	8.69
135	224	8.50
136	225	8.05
137	226	7.71
138	227	7.53
139	228	7.24
140	229	6.68
141	230	6.49
142	231	6.24
143	232	6.19
144	233	6.08
145	234	6.16
146	235	6.27
147	236	6.89
148	237	7.08
149	238	7.61
150	239	7.75
151	240	8.26
152	241	8.19
153	242	8.15
154	243	7.84
155	244	7.62
156	245	7.35
157	246	7.36
158	247	7.12
159	248	7.10
160	249	6.86
161	250	6.94
162	251	6.74
163	252	6.81
164	253	6.59
165	254	6.50
166	255	6.27
167	256	6.64
168	257	6.91
169	258	7.31
170	259	7.48
171	260	7.85

Calculated Fission-Barrier Heights

N	A	$B_{\rm f}$ (MeV)
172	261	8.01
173	262	7.97
174	263	8.11
175	264	8.77
176	265	9.20
177	266	9.78
178	267	9.77
179	268	10.24
180	269	10.27
181	270	10.81
182	271	10.79
183	272	11.06
184	273	10.58
185	274	9.60
186	275	8.99
187	276	8.10
188	277	7.55
189	278	7.79
190	279	7.60
191	280	7.64
192	281	7.23
193	282	6.84
194	283	6.29
195	284	5.97
196	285	5.56
197	286	5.30
198	287	4.86
199	288	4.39
200	289	3.81
201	290	3.41
202	291	3.00
203	292	2.82
204	293	2.51
205	294	2.65
206	295	2.70
$Z = 90$ (Th)		
108	198	2.53
109	199	2.77
110	200	2.69
111	201	2.89
112	202	2.86
113	203	3.61
114	204	3.85
115	205	4.79
116	206	5.44
117	207	6.43
118	208	7.57
119	209	8.55
120	210	9.39
121	211	10.11
122	212	10.66
123	213	11.34
124	214	11.68
125	215	12.34
126	216	12.17
127	217	11.02
128	218	9.99
129	219	9.17
130	220	8.45
131	221	8.27

Calculated Fission-Barrier Heights

N	A	B_{f} (MeV)
132	222	7.99
133	223	8.20
134	224	7.85
135	225	7.59
136	226	7.20
137	227	6.98
138	228	6.52
139	229	6.06
140	230	5.66
141	231	5.55
142	232	5.44
143	233	5.47
144	234	5.38
145	235	5.80
146	236	6.04
147	237	6.64
148	238	6.84
149	239	7.35
150	240	7.53
151	241	8.00
152	242	7.97
153	243	7.89
154	244	7.61
155	245	7.36
156	246	6.94
157	247	7.12
158	248	6.88
159	249	6.72
160	250	6.59
161	251	6.63
162	252	6.40
163	253	6.22
164	254	6.07
165	255	5.86
166	256	5.53
167	257	5.88
168	258	6.08
169	259	6.39
170	260	6.61
171	261	7.05
172	262	7.04
173	263	6.88
174	264	7.01
175	265	7.60
176	266	8.00
177	267	8.52
178	268	8.73
179	269	9.33
180	270	9.38
181	271	9.84
182	272	9.87
183	273	10.09
184	274	9.65
185	275	8.66
186	276	8.08
187	277	7.27
188	278	6.84
189	279	7.06
190	280	6.90
191	281	6.97

Calculated Fission-Barrier Heights

N	A	B_{f} (MeV)
192	282	6.66
193	283	6.31
194	284	5.87
195	285	5.76
196	286	5.40
197	287	5.14
198	288	4.74
199	289	4.22
200	290	3.62
201	291	3.33
202	292	3.05
203	293	2.91
204	294	2.67
205	295	2.78
206	296	2.87
207	297	3.12
208	298	3.17
209	299	3.03
$Z = 91$ (Pa)		
109	200	2.18
110	201	2.08
111	202	2.06
112	203	2.08
113	204	2.64
114	205	3.04
115	206	4.01
116	207	4.74
117	208	5.62
118	209	6.55
119	210	7.44
120	211	8.19
121	212	8.97
122	213	9.33
123	214	9.97
124	215	10.35
125	216	10.93
126	217	10.81
127	218	9.68
128	219	8.60
129	220	8.20
130	221	7.55
131	222	6.93
132	223	6.91
133	224	7.03
134	225	6.84
135	226	6.91
136	227	6.51
137	228	6.26
138	229	5.59
139	230	5.28
140	231	4.99
141	232	4.97
142	233	4.99
143	234	5.13
144	235	5.33
145	236	5.76
146	237	5.99
147	238	6.57
148	239	6.72
149	240	7.27

Calculated Fission-Barrier Heights

N	A	B_{f} (MeV)
150	241	7.43
151	242	7.87
152	243	7.79
153	244	7.76
154	245	7.40
155	246	7.12
156	247	6.89
157	248	6.91
158	249	6.66
159	250	6.67
160	251	6.34
161	252	6.35
162	253	6.05
163	254	5.87
164	255	5.58
165	256	5.35
166	257	5.17
167	258	5.30
168	259	5.42
169	260	5.64
170	261	5.84
171	262	6.24
172	263	6.24
173	264	6.30
174	265	6.33
175	266	6.82
176	267	7.14
177	268	7.59
178	269	7.93
179	270	8.46
180	271	8.49
181	272	8.98
182	273	8.91
183	274	9.13
184	275	8.65
185	276	7.57
186	277	7.09
187	278	6.41
188	279	6.23
189	280	6.35
190	281	6.20
191	282	6.31
192	283	6.01
193	284	6.11
194	285	5.93
195	286	5.85
196	287	5.46
197	288	5.23
198	289	4.76
199	290	4.30
200	291	3.85
201	292	3.60
202	293	3.11
203	294	2.98
204	295	2.83
205	296	2.99
206	297	3.07
207	298	3.34
208	299	3.32
209	300	3.39

Calculated Fission-Barrier Heights

N	A	B_{f} (MeV)
210	301	3.17
211	302	3.06
$Z = 92$ (U)		
111	203	1.21
112	204	1.14
113	205	1.74
114	206	2.27
115	207	3.24
116	208	3.84
117	209	4.59
118	210	5.44
119	211	6.51
120	212	7.18
121	213	7.85
122	214	8.30
123	215	8.82
124	216	9.25
125	217	9.78
126	218	9.67
127	219	8.54
128	220	7.62
129	221	7.06
130	222	6.46
131	223	5.87
132	224	5.65
133	225	5.81
134	226	5.59
135	227	5.48
136	228	5.13
137	229	4.94
138	230	4.28
139	231	4.46
140	232	4.72
141	233	4.79
142	234	4.89
143	235	4.87
144	236	5.03
145	237	5.43
146	238	5.63
147	239	6.21
148	240	6.38
149	241	6.93
150	242	7.10
151	243	7.50
152	244	7.46
153	245	7.39
154	246	7.21
155	247	7.03
156	248	6.64
157	249	6.57
158	250	6.31
159	251	6.37
160	252	6.04
161	253	6.00
162	254	5.74
163	255	5.48
164	256	5.02
165	257	4.78
166	258	4.61
167	259	4.64

Calculated Fission-Barrier Heights

N	A	B_{f} (MeV)
168	260	4.70
169	261	4.89
170	262	4.95
171	263	5.33
172	264	5.59
173	265	5.67
174	266	5.74
175	267	6.11
176	268	6.60
177	269	7.03
178	270	7.09
179	271	7.58
180	272	7.64
181	273	8.06
182	274	8.06
183	275	8.26
184	276	7.72
185	277	6.71
186	278	6.26
187	279	5.64
188	280	5.51
189	281	5.59
190	282	5.50
191	283	5.59
192	284	5.41
193	285	5.63
194	286	5.69
195	287	5.50
196	288	5.09
197	289	4.86
198	290	4.44
199	291	4.28
200	292	3.93
201	293	3.84
202	294	3.33
203	295	3.12
204	296	2.95
205	297	3.02
206	298	3.16
207	299	3.40
208	300	3.38
209	301	3.33
210	302	3.20
211	303	3.24
212	304	3.23
213	305	3.44
$Z = 93$ (Np)		
113	206	1.16
114	207	1.66
115	208	2.52
116	209	3.05
117	210	3.72
118	211	4.49
119	212	5.21
120	213	6.09
121	214	6.67
122	215	7.00
123	216	7.52
124	217	7.83
125	218	8.28

Calculated Fission-Barrier Heights

N	A	B_{f} (MeV)
126	219	8.26
127	220	7.32
128	221	6.47
129	222	6.01
130	223	5.28
131	224	4.96
132	225	4.43
133	226	4.17
134	227	3.78
135	228	3.70
136	229	3.81
137	230	3.81
138	231	3.81
139	232	4.14
140	233	4.37
141	234	4.63
142	235	4.83
143	236	4.81
144	237	4.94
145	238	5.36
146	239	5.57
147	240	6.01
148	241	6.15
149	242	6.76
150	243	6.87
151	244	7.35
152	245	7.27
153	246	7.39
154	247	7.09
155	248	6.89
156	249	6.46
157	250	6.35
158	251	6.01
159	252	5.87
160	253	5.72
161	254	5.64
162	255	5.39
163	256	5.12
164	257	4.58
165	258	4.27
166	259	4.06
167	260	4.04
168	261	4.04
169	262	4.18
170	263	4.17
171	264	4.76
172	265	5.12
173	266	5.23
174	267	5.29
175	268	5.78
176	269	6.18
177	270	6.60
178	271	6.51
179	272	6.68
180	273	6.56
181	274	7.01
182	275	6.93
183	276	7.01
184	277	6.43
185	278	5.72

Calculated Fission-Barrier Heights

N	A	B_{f} (MeV)
186	279	5.19
187	280	5.08
188	281	4.79
189	282	5.00
190	283	4.90
191	284	5.12
192	285	5.11
193	286	5.37
194	287	5.26
195	288	5.43
196	289	4.96
197	290	4.73
198	291	4.52
199	292	4.34
200	293	4.09
201	294	3.93
202	295	3.54
203	296	3.26
204	297	3.07
205	298	3.22
206	299	3.26
207	300	3.44
208	301	3.40
209	302	3.48
210	303	3.50
211	304	3.66
212	305	3.65
213	306	3.85
214	307	3.83
215	308	4.08
$Z = 94$ (Pu)		
115	209	1.72
116	210	2.25
117	211	3.05
118	212	3.59
119	213	4.39
120	214	5.09
121	215	5.70
122	216	6.01
123	217	6.45
124	218	6.78
125	219	7.28
126	220	7.34
127	221	6.44
128	222	5.62
129	223	5.07
130	224	4.47
131	225	4.24
132	226	3.74
133	227	3.43
134	228	2.93
135	229	2.95
136	230	3.07
137	231	3.05
138	232	3.23
139	233	3.50
140	234	3.83
141	235	4.09
142	236	4.49
143	237	5.00

Calculated Fission-Barrier Heights

N	A	B_{f} (MeV)
144	238	5.26
145	239	5.74
146	240	5.98
147	241	6.35
148	242	6.41
149	243	6.66
150	244	6.59
151	245	6.93
152	246	7.07
153	247	7.12
154	248	6.80
155	249	6.59
156	250	6.17
157	251	5.94
158	252	5.63
159	253	5.64
160	254	5.41
161	255	5.40
162	256	5.14
163	257	4.83
164	258	4.27
165	259	4.04
166	260	3.96
167	261	4.09
168	262	3.94
169	263	4.10
170	264	3.91
171	265	4.24
172	266	4.59
173	267	4.63
174	268	4.70
175	269	5.27
176	270	5.74
177	271	6.21
178	272	6.18
179	273	6.32
180	274	6.20
181	275	6.35
182	276	6.15
183	277	6.07
184	278	5.72
185	279	4.96
186	280	4.43
187	281	4.12
188	282	4.07
189	283	4.29
190	284	4.24
191	285	4.47
192	286	4.49
193	287	4.69
194	288	4.59
195	289	4.73
196	290	4.65
197	291	4.68
198	292	4.47
199	293	4.32
200	294	4.03
201	295	3.84
202	296	3.51
203	297	3.34

Calculated Fission-Barrier Heights

N	A	B_{f} (MeV)
204	298	3.04
205	299	3.18
206	300	3.28
207	301	3.58
208	302	3.69
209	303	3.89
210	304	3.96
211	305	4.15
212	306	4.22
213	307	4.40
214	308	4.34
215	309	4.36
216	310	4.12
217	311	4.20
218	312	4.10
$Z = 95$ (Am)		
117	212	2.40
118	213	3.13
119	214	3.57
120	215	4.03
121	216	4.56
122	217	4.81
123	218	5.32
124	219	5.60
125	220	6.19
126	221	6.23
127	222	5.46
128	223	4.74
129	224	4.33
130	225	3.80
131	226	3.61
132	227	2.91
133	228	2.71
134	229	2.50
135	230	2.46
136	231	2.51
137	232	2.65
138	233	2.79
139	234	3.27
140	235	3.80
141	236	4.33
142	237	4.80
143	238	5.34
144	239	5.66
145	240	6.12
146	241	6.34
147	242	6.72
148	243	6.80
149	244	6.99
150	245	6.80
151	246	6.88
152	247	6.83
153	248	6.91
154	249	6.59
155	250	6.37
156	251	5.87
157	252	5.79
158	253	5.41
159	254	5.45
160	255	5.19

Calculated Fission-Barrier Heights

N	A	B_{f} (MeV)
161	256	5.17
162	257	4.89
163	258	4.59
164	259	4.07
165	260	4.00
166	261	3.86
167	262	3.99
168	263	3.92
169	264	4.17
170	265	4.01
171	266	4.24
172	267	4.48
173	268	4.51
174	269	4.48
175	270	4.88
176	271	5.26
177	272	5.62
178	273	5.56
179	274	5.81
180	275	5.61
181	276	5.85
182	277	5.49
183	278	5.08
184	279	4.64
185	280	4.08
186	281	3.52
187	282	3.63
188	283	3.46
189	284	3.71
190	285	3.74
191	286	3.97
192	287	3.95
193	288	4.20
194	289	4.19
195	290	4.69
196	291	4.61
197	292	4.76
198	293	4.61
199	294	4.40
200	295	4.15
201	296	3.96
202	297	3.66
203	298	3.53
204	299	3.34
205	300	3.60
206	301	3.69
207	302	3.99
208	303	4.11
209	304	4.33
210	305	4.43
211	306	4.62
212	307	4.64
213	308	4.66
214	309	4.44
215	310	4.42
216	311	4.20
217	312	4.25
218	313	4.16
219	314	4.18
220	315	4.01

Calculated Fission-Barrier Heights

N	A	B_{f} (MeV)
$Z = 96$ (Cm)		
119	215	3.04
120	216	3.31
121	217	3.78
122	218	4.09
123	219	4.59
124	220	4.99
125	221	5.62
126	222	5.64
127	223	4.85
128	224	4.16
129	225	3.69
130	226	3.02
131	227	2.68
132	228	2.11
133	229	1.99
134	230	1.87
135	231	2.00
136	232	2.10
137	233	2.24
138	234	2.61
139	235	3.23
140	236	3.81
141	237	4.34
142	238	4.92
143	239	5.48
144	240	5.85
145	241	6.32
146	242	6.56
147	243	6.97
148	244	6.92
149	245	7.13
150	246	7.02
151	247	7.11
152	248	6.80
153	249	6.56
154	250	6.25
155	251	6.09
156	252	5.68
157	253	5.57
158	254	5.20
159	255	5.22
160	256	5.00
161	257	4.97
162	258	4.69
163	259	4.37
164	260	4.15
165	261	4.07
166	262	3.88
167	263	3.92
168	264	3.85
169	265	4.01
170	266	3.99
171	267	4.32
172	268	4.40
173	269	4.53
174	270	4.45
175	271	4.65
176	272	4.95
177	273	5.22

Calculated Fission-Barrier Heights

N	A	B_{f} (MeV)
178	274	5.17
179	275	5.45
180	276	5.33
181	277	5.53
182	278	5.34
183	279	5.13
184	280	4.40
185	281	3.31
186	282	2.84
187	283	2.72
188	284	2.59
189	285	2.85
190	286	2.81
191	287	3.05
192	288	3.14
193	289	3.41
194	290	3.58
195	291	3.97
196	292	4.14
197	293	4.45
198	294	4.26
199	295	4.26
200	296	4.01
201	297	3.89
202	298	3.61
203	299	3.78
204	300	3.87
205	301	4.02
206	302	4.11
207	303	4.38
208	304	4.49
209	305	4.70
210	306	4.84
211	307	4.91
212	308	4.75
213	309	4.72
214	310	4.51
215	311	4.48
216	312	4.34
217	313	4.42
218	314	4.31
219	315	4.28
220	316	4.14
221	317	4.18
222	318	3.97
$Z = 97$ (Bk)		
121	218	2.90
122	219	3.16
123	220	3.65
124	221	3.93
125	222	4.49
126	223	4.66
127	224	3.98
128	225	3.44
129	226	2.84
130	227	2.17
131	228	2.17
132	229	1.93
133	230	1.72
134	231	1.64

Calculated Fission-Barrier Heights

N	A	B_{f} (MeV)
135	232	1.81
136	233	1.94
137	234	2.27
138	235	2.71
139	236	3.37
140	237	3.99
141	238	4.55
142	239	5.16
143	240	5.76
144	241	6.14
145	242	6.63
146	243	6.91
147	244	7.28
148	245	7.22
149	246	7.32
150	247	7.18
151	248	7.27
152	249	7.00
153	250	6.59
154	251	6.21
155	252	6.01
156	253	5.59
157	254	5.50
158	255	5.10
159	256	5.09
160	257	4.80
161	258	4.58
162	259	4.51
163	260	4.42
164	261	4.21
165	262	4.03
166	263	3.80
167	264	3.80
168	265	3.72
169	266	3.74
170	267	3.70
171	268	4.07
172	269	4.09
173	270	4.32
174	271	4.19
175	272	4.33
176	273	4.49
177	274	4.77
178	275	4.69
179	276	4.93
180	277	4.71
181	278	4.86
182	279	4.70
183	280	4.61
184	281	3.87
185	282	2.95
186	283	2.17
187	284	2.09
188	285	2.00
189	286	2.29
190	287	2.43
191	288	2.70
192	289	2.84
193	290	3.13
194	291	3.33

Calculated Fission-Barrier Heights

N	A	B_{f} (MeV)
195	292	3.68
196	293	3.85
197	294	4.21
198	295	4.10
199	296	4.14
200	297	3.98
201	298	4.05
202	299	3.99
203	300	4.17
204	301	4.20
205	302	4.42
206	303	4.43
207	304	4.59
208	305	4.66
209	306	4.95
210	307	4.90
211	308	4.99
212	309	4.84
213	310	4.82
214	311	4.70
215	312	4.61
216	313	4.44
217	314	4.53
218	315	4.45
219	316	4.45
220	317	4.28
221	318	4.31
222	319	4.08
223	320	4.06
224	321	3.78
$Z = 98$ (Cf)		
123	221	3.09
124	222	3.39
125	223	3.89
126	224	4.04
127	225	3.41
128	226	2.65
129	227	1.99
130	228	1.39
131	229	1.58
132	230	1.58
133	231	1.67
134	232	1.57
135	233	1.50
136	234	1.64
137	235	2.10
138	236	2.69
139	237	3.34
140	238	4.01
141	239	4.64
142	240	5.22
143	241	5.83
144	242	6.16
145	243	6.55
146	244	6.69
147	245	6.99
148	246	7.16
149	247	7.35
150	248	7.24
151	249	7.31

Calculated Fission-Barrier Heights

N	A	B_{f} (MeV)
152	250	7.09
153	251	6.64
154	252	6.07
155	253	5.62
156	254	5.27
157	255	5.21
158	256	4.82
159	257	4.56
160	258	4.43
161	259	4.57
162	260	4.64
163	261	4.54
164	262	4.30
165	263	4.06
166	264	3.81
167	265	3.77
168	266	3.68
169	267	3.64
170	268	3.65
171	269	3.98
172	270	4.09
173	271	4.27
174	272	4.18
175	273	4.11
176	274	4.30
177	275	4.56
178	276	4.50
179	277	4.68
180	278	4.47
181	279	4.65
182	280	4.53
183	281	4.47
184	282	3.82
185	283	2.86
186	284	2.00
187	285	1.50
188	286	1.27
189	287	1.51
190	288	1.70
191	289	2.00
192	290	2.21
193	291	2.52
194	292	2.69
195	293	3.05
196	294	3.21
197	295	3.59
198	296	3.73
199	297	3.94
200	298	3.85
201	299	4.04
202	300	4.10
203	301	4.27
204	302	4.28
205	303	4.43
206	304	4.48
207	305	4.62
208	306	4.64
209	307	4.86
210	308	4.81
211	309	4.91

Calculated Fission-Barrier Heights

N	A	B_{f} (MeV)
212	310	4.76
213	311	4.83
214	312	4.56
215	313	4.62
216	314	4.47
217	315	4.56
218	316	4.50
219	317	4.49
220	318	4.30
221	319	4.30
222	320	4.18
223	321	4.11
224	322	3.86
225	323	3.84
226	324	4.02
227	325	3.86
$Z = 99$ (Es)		
125	224	2.29
126	225	2.51
127	226	1.80
128	227	0.98
129	228	1.01
130	229	0.70
131	230	1.30
132	231	1.30
133	232	1.44
134	233	1.46
135	234	1.56
136	235	1.83
137	236	2.38
138	237	2.96
139	238	3.59
140	239	4.32
141	240	4.95
142	241	5.32
143	242	5.70
144	243	5.98
145	244	6.28
146	245	6.53
147	246	6.90
148	247	7.07
149	248	7.44
150	249	7.38
151	250	7.48
152	251	7.24
153	252	6.79
154	253	6.22
155	254	5.67
156	255	5.05
157	256	5.01
158	257	4.50
159	258	4.32
160	259	4.43
161	260	4.64
162	261	4.68
163	262	4.60
164	263	4.32
165	264	4.06
166	265	3.81
167	266	3.71

Calculated Fission-Barrier Heights

N	A	B_{f} (MeV)
168	267	3.60
169	268	3.51
170	269	3.50
171	270	3.82
172	271	3.85
173	272	4.08
174	273	3.96
175	274	4.06
176	275	3.82
177	276	4.17
178	277	4.10
179	278	4.27
180	279	4.02
181	280	4.12
182	281	3.95
183	282	3.99
184	283	3.39
185	284	2.60
186	285	1.75
187	286	1.46
188	287	1.21
189	288	1.40
190	289	1.63
191	290	1.80
192	291	2.06
193	292	2.39
194	293	2.57
195	294	2.77
196	295	3.00
197	296	3.22
198	297	3.42
199	298	3.76
200	299	3.95
201	300	4.21
202	301	4.26
203	302	4.42
204	303	4.42
205	304	4.53
206	305	4.59
207	306	4.70
208	307	4.67
209	308	4.73
210	309	4.72
211	310	4.80
212	311	4.68
213	312	4.78
214	313	4.67
215	314	4.70
216	315	4.57
217	316	4.67
218	317	4.55
219	318	4.57
220	319	4.39
221	320	4.56
222	321	4.39
223	322	4.25
224	323	4.01
225	324	4.01
226	325	3.83
227	326	4.12

Calculated Fission-Barrier Heights

N	A	B_{f} (MeV)
228	327	3.74
229	328	3.91
$Z = 100$ (Fm)		
126	226	2.84
127	227	2.08
128	228	0.80
129	229	0.90
130	230	0.79
131	231	0.85
132	232	1.25
133	233	1.39
134	234	1.46
135	235	1.56
136	236	1.87
137	237	2.39
138	238	2.88
139	239	3.49
140	240	4.14
141	241	4.50
142	242	4.88
143	243	5.29
144	244	5.57
145	245	5.94
146	246	6.13
147	247	6.48
148	248	6.73
149	249	7.12
150	250	7.22
151	251	7.38
152	252	7.16
153	253	6.74
154	254	6.24
155	255	5.72
156	256	5.11
157	257	4.75
158	258	4.52
159	259	4.54
160	260	4.62
161	261	4.68
162	262	4.82
163	263	4.75
164	264	4.49
165	265	4.23
166	266	3.94
167	267	3.74
168	268	3.60
169	269	3.58
170	270	3.58
171	271	3.87
172	272	3.91
173	273	4.14
174	274	4.06
175	275	4.12
176	276	3.77
177	277	4.13
178	278	4.06
179	279	4.25
180	280	4.03
181	281	4.13
182	282	3.93

Calculated Fission-Barrier Heights

N	A	B_{f} (MeV)
183	283	3.96
184	284	3.43
185	285	2.58
186	286	1.71
187	287	1.29
188	288	1.17
189	289	1.31
190	290	1.61
191	291	1.85
192	292	2.13
193	293	2.47
194	294	2.66
195	295	2.87
196	296	2.99
197	297	3.23
198	298	3.48
199	299	3.86
200	300	4.00
201	301	4.23
202	302	4.29
203	303	4.44
204	304	4.34
205	305	4.41
206	306	4.46
207	307	4.52
208	308	4.41
209	309	4.50
210	310	4.50
211	311	4.60
212	312	4.52
213	313	4.66
214	314	4.54
215	315	4.63
216	316	4.50
217	317	4.63
218	318	4.55
219	319	4.57
220	320	4.58
221	321	4.76
222	322	4.51
223	323	4.53
224	324	4.20
225	325	4.27
226	326	4.11
227	327	4.51
228	328	4.25
229	329	4.32
230	330	3.98
$Z = 101$ (Md)		
128	229	0.70
129	230	0.84
130	231	0.74
131	232	0.89
132	233	1.03
133	234	1.30
134	235	1.57
135	236	1.72
136	237	2.01
137	238	2.49
138	239	2.86

Calculated Fission-Barrier Heights

N	A	B_{f} (MeV)
139	240	3.25
140	241	3.64
141	242	4.09
142	243	4.46
143	244	4.80
144	245	5.11
145	246	5.47
146	247	5.74
147	248	6.03
148	249	6.24
149	250	6.70
150	251	6.98
151	252	7.23
152	253	7.01
153	254	6.61
154	255	6.13
155	256	5.69
156	257	5.09
157	258	4.84
158	259	4.67
159	260	4.92
160	261	4.99
161	262	5.05
162	263	5.12
163	264	4.89
164	265	4.59
165	266	4.31
166	267	3.99
167	268	3.75
168	269	3.57
169	270	3.54
170	271	3.47
171	272	3.75
172	273	3.77
173	274	3.99
174	275	3.92
175	276	4.00
176	277	3.67
177	278	3.85
178	279	3.72
179	280	3.95
180	281	3.72
181	282	3.78
182	283	3.52
183	284	3.60
184	285	3.11
185	286	2.37
186	287	1.53
187	288	1.26
188	289	1.15
189	290	1.38
190	291	1.71
191	292	1.99
192	293	2.28
193	294	2.63
194	295	2.69
195	296	2.95
196	297	3.12
197	298	3.49
198	299	3.74

Calculated Fission-Barrier Heights

N	A	$B_{\rm f}$ (MeV)
199	300	3.97
200	301	4.13
201	302	4.36
202	303	4.31
203	304	4.46
204	305	4.38
205	306	4.39
206	307	4.41
207	308	4.39
208	309	4.29
209	310	4.32
210	311	4.36
211	312	4.50
212	313	4.46
213	314	4.59
214	315	4.54
215	316	4.63
216	317	4.52
217	318	4.68
218	319	4.62
219	320	4.71
220	321	4.75
221	322	4.90
222	323	4.81
223	324	4.79
224	325	4.47
225	326	4.57
226	327	4.42
227	328	4.91
228	329	4.62
229	330	4.66
$Z = 102$ (No)		
130	232	0.83
131	233	0.75
132	234	0.97
133	235	1.03
134	236	1.27
135	237	1.59
136	238	2.05
137	239	2.35
138	240	2.55
139	241	2.82
140	242	3.18
141	243	3.58
142	244	3.94
143	245	4.32
144	246	4.62
145	247	4.98
146	248	5.24
147	249	5.61
148	250	5.83
149	251	6.25
150	252	6.50
151	253	6.93
152	254	6.76
153	255	6.38
154	256	5.94
155	257	5.52
156	258	4.98
157	259	5.00

Calculated Fission-Barrier Heights

N	A	B_{f} (MeV)
158	260	4.93
159	261	5.26
160	262	5.11
161	263	5.26
162	264	5.36
163	265	5.40
164	266	5.01
165	267	4.72
166	268	4.19
167	269	3.96
168	270	3.74
169	271	3.69
170	272	3.66
171	273	3.93
172	274	3.95
173	275	4.22
174	276	4.11
175	277	4.22
176	278	3.86
177	279	3.93
178	280	3.84
179	281	4.07
180	282	3.80
181	283	4.02
182	284	3.72
183	285	3.80
184	286	3.21
185	287	2.41
186	288	1.61
187	289	1.29
188	290	0.98
189	291	1.20
190	292	1.62
191	293	1.89
192	294	2.19
193	295	2.54
194	296	2.62
195	297	2.95
196	298	3.17
197	299	3.54
198	300	3.66
199	301	3.86
200	302	4.06
201	303	4.30
202	304	4.19
203	305	4.42
204	306	4.23
205	307	4.24
206	308	4.12
207	309	4.12
208	310	4.11
209	311	4.12
210	312	4.15
211	313	4.30
212	314	4.27
213	315	4.39
214	316	4.38
215	317	4.49
216	318	4.44
217	319	4.58

Calculated Fission-Barrier Heights

N	A	B_{f} (MeV)
218	320	4.56
219	321	4.64
220	322	4.78
221	323	5.08
222	324	4.99
223	325	4.98
224	326	4.82
225	327	5.06
226	328	5.00
227	329	5.50
228	330	5.07
$Z = 103$ (Lr)		
132	235	1.07
133	236	1.18
134	237	1.44
135	238	1.75
136	239	1.95
137	240	2.12
138	241	2.28
139	242	2.46
140	243	2.79
141	244	3.18
142	245	3.49
143	246	3.89
144	247	4.19
145	248	4.50
146	249	4.81
147	250	5.26
148	251	5.55
149	252	5.97
150	253	6.27
151	254	6.70
152	255	6.60
153	256	6.27
154	257	5.90
155	258	5.52
156	259	5.21
157	260	5.39
158	261	5.37
159	262	5.52
160	263	5.48
161	264	5.73
162	265	5.97
163	266	6.03
164	267	5.63
165	268	5.22
166	269	4.81
167	270	4.36
168	271	3.96
169	272	3.78
170	273	3.69
171	274	3.94
172	275	3.94
173	276	4.21
174	277	4.13
175	278	4.23
176	279	3.87
177	280	3.76
178	281	3.65
179	282	3.91

Calculated Fission-Barrier Heights

N	A	$B_{\rm f}$ (MeV)
180	283	3.62
181	284	3.86
182	285	3.58
183	286	3.61
184	287	2.99
185	288	2.26
186	289	1.61
187	290	1.32
188	291	1.04
189	292	1.22
190	293	1.51
191	294	1.89
192	295	2.19
193	296	2.51
194	297	2.68
195	298	2.93
196	299	3.24
197	300	3.59
198	301	3.74
199	302	4.01
200	303	4.08
201	304	4.27
202	305	4.22
203	306	4.39
204	307	4.36
205	308	4.23
206	309	4.14
207	310	4.03
208	311	3.99
209	312	4.07
210	313	4.06
211	314	4.20
212	315	4.21
213	316	4.34
214	317	4.38
215	318	4.56
216	319	4.53
217	320	4.68
218	321	4.63
219	322	4.77
220	323	4.90
221	324	5.28
222	325	5.18
223	326	5.28
224	327	5.18
225	328	5.41
226	329	5.31
227	330	6.00
$Z = 104$ (Rf)		
134	238	1.11
135	239	1.28
136	240	1.53
137	241	1.67
138	242	1.82
139	243	2.01
140	244	2.28
141	245	2.54
142	246	2.95
143	247	3.33
144	248	3.64

Calculated Fission-Barrier Heights

N	A	B_{f} (MeV)
145	249	3.95
146	250	4.36
147	251	4.76
148	252	5.09
149	253	5.53
150	254	5.87
151	255	6.24
152	256	6.26
153	257	6.02
154	258	5.65
155	259	5.49
156	260	5.36
157	261	5.56
158	262	5.59
159	263	5.61
160	264	5.79
161	265	6.27
162	266	6.43
163	267	6.43
164	268	6.03
165	269	5.60
166	270	5.10
167	271	4.72
168	272	4.28
169	273	4.06
170	274	3.82
171	275	4.06
172	276	4.10
173	277	4.43
174	278	4.37
175	279	4.45
176	280	4.10
177	281	4.17
178	282	4.12
179	283	4.43
180	284	4.22
181	285	4.19
182	286	3.95
183	287	3.96
184	288	3.23
185	289	2.38
186	290	1.80
187	291	1.37
188	292	1.11
189	293	1.24
190	294	1.27
191	295	1.61
192	296	1.94
193	297	2.24
194	298	2.55
195	299	2.70
196	300	3.12
197	301	3.42
198	302	3.57
199	303	3.80
200	304	3.90
201	305	4.09
202	306	4.11
203	307	4.34
204	308	4.18

Calculated Fission-Barrier Heights

N	A	B_{f} (MeV)
205	309	4.11
206	310	4.01
207	311	3.93
208	312	3.86
209	313	3.89
210	314	3.88
211	315	4.01
212	316	4.03
213	317	4.24
214	318	4.31
215	319	4.50
216	320	4.46
217	321	4.61
218	322	4.56
219	323	4.93
220	324	5.09
221	325	5.41
222	326	5.40
223	327	5.58
224	328	5.55
225	329	5.76
226	330	5.68
$Z = 105$ (Db)		
136	241	1.31
137	242	1.44
138	243	1.55
139	244	1.68
140	245	1.94
141	246	2.18
142	247	2.59
143	248	2.88
144	249	3.21
145	250	3.53
146	251	4.01
147	252	4.44
148	253	4.81
149	254	5.26
150	255	5.67
151	256	6.05
152	257	6.22
153	258	6.01
154	259	5.76
155	260	5.81
156	261	5.76
157	262	5.94
158	263	5.90
159	264	6.08
160	265	6.36
161	266	6.80
162	267	6.99
163	268	7.00
164	269	6.59
165	270	6.13
166	271	5.62
167	272	5.18
168	273	4.69
169	274	4.45
170	275	4.00
171	276	4.16
172	277	4.21

Calculated Fission-Barrier Heights

N	A	B_{f} (MeV)
173	278	4.48
174	279	4.48
175	280	4.56
176	281	4.35
177	282	4.31
178	283	4.20
179	284	4.59
180	285	4.37
181	286	4.40
182	287	3.86
183	288	3.79
184	289	3.06
185	290	2.35
186	291	1.78
187	292	0.90
188	293	1.11
189	294	1.23
190	295	1.16
191	296	1.48
192	297	1.82
193	298	2.17
194	299	2.44
195	300	2.75
196	301	3.10
197	302	3.38
198	303	3.48
199	304	3.73
200	305	3.82
201	306	4.07
202	307	4.14
203	308	4.21
204	309	4.09
205	310	3.96
206	311	3.89
207	312	3.90
208	313	3.82
209	314	3.87
210	315	3.89
211	316	4.05
212	317	4.10
213	318	4.31
214	319	4.31
215	320	4.40
216	321	4.47
217	322	4.60
218	323	4.85
219	324	5.30
220	325	5.43
221	326	5.77
222	327	5.74
223	328	5.99
224	329	5.92
225	330	6.18
$Z = 106$ (Sg)		
138	244	1.15
139	245	1.27
140	246	1.44
141	247	1.73
142	248	2.11
143	249	2.38

Calculated Fission-Barrier Heights

N	A	B_{f} (MeV)
144	250	2.67
145	251	3.16
146	252	3.59
147	253	4.02
148	254	4.44
149	255	4.86
150	256	5.30
151	257	5.70
152	258	5.93
153	259	5.82
154	260	5.84
155	261	5.88
156	262	5.91
157	263	6.17
158	264	5.98
159	265	6.27
160	266	6.69
161	267	7.08
162	268	7.29
163	269	7.30
164	270	6.92
165	271	6.48
166	272	5.94
167	273	5.48
168	274	4.96
169	275	4.70
170	276	4.39
171	277	4.43
172	278	4.39
173	279	4.63
174	280	4.63
175	281	5.06
176	282	4.82
177	283	4.83
178	284	4.75
179	285	5.05
180	286	4.91
181	287	4.91
182	288	4.44
183	289	4.15
184	290	3.42
185	291	2.60
186	292	1.97
187	293	0.02
188	294	0.02
189	295	1.01
190	296	1.01
191	297	1.10
192	298	1.42
193	299	1.87
194	300	2.14
195	301	2.45
196	302	2.83
197	303	3.12
198	304	3.25
199	305	3.52
200	306	3.63
201	307	3.85
202	308	3.92
203	309	4.03

Calculated Fission-Barrier Heights

N	A	B_{f} (MeV)
204	310	3.92
205	311	3.94
206	312	3.76
207	313	3.72
208	314	3.69
209	315	3.82
210	316	3.85
211	317	4.04
212	318	4.10
213	319	4.19
214	320	4.13
215	321	4.22
216	322	4.21
217	323	4.38
218	324	4.87
219	325	5.42
220	326	5.55
221	327	5.91
222	328	5.94
223	329	6.19
224	330	6.13
$Z = 107$ (Ns)		
140	247	1.13
141	248	1.33
142	249	1.70
143	250	1.91
144	251	2.45
145	252	2.88
146	253	3.27
147	254	3.74
148	255	4.10
149	256	4.54
150	257	5.00
151	258	5.41
152	259	5.66
153	260	5.87
154	261	6.01
155	262	6.20
156	263	6.20
157	264	6.39
158	265	6.34
159	266	6.71
160	267	6.97
161	268	7.20
162	269	7.60
163	270	7.69
164	271	7.39
165	272	6.94
166	273	6.38
167	274	5.93
168	275	5.30
169	276	5.13
170	277	4.80
171	278	4.82
172	279	4.73
173	280	5.05
174	281	5.07
175	282	5.39
176	283	5.10
177	284	5.12

Calculated Fission-Barrier Heights

N	A	B_{f} (MeV)
178	285	5.03
179	286	5.45
180	287	5.29
181	288	5.36
182	289	4.93
183	290	4.74
184	291	4.15
185	292	2.66
186	293	2.70
187	294	0.02
188	295	0.02
189	296	0.87
190	297	1.02
191	298	0.84
192	299	1.25
193	300	1.67
194	301	1.93
195	302	2.32
196	303	2.69
197	304	2.96
198	305	3.08
199	306	3.29
200	307	3.39
201	308	3.62
202	309	3.75
203	310	3.80
204	311	3.79
205	312	3.75
206	313	3.61
207	314	3.57
208	315	3.51
209	316	3.69
210	317	3.76
211	318	4.00
212	319	3.99
213	320	4.13
214	321	4.03
215	322	4.07
216	323	4.13
217	324	4.61
218	325	4.97
219	326	5.52
220	327	5.69
221	328	6.02
222	329	6.15
223	330	6.50
$Z = 108$ (Hs)		
142	250	1.02
143	251	1.55
144	252	1.97
145	253	2.39
146	254	2.82
147	255	3.22
148	256	3.64
149	257	4.01
150	258	4.54
151	259	4.93
152	260	5.39
153	261	5.65
154	262	5.88

Calculated Fission-Barrier Heights

N	A	B_{f} (MeV)
155	263	6.01
156	264	6.13
157	265	6.26
158	266	6.26
159	267	6.47
160	268	6.59
161	269	7.04
162	270	7.37
163	271	7.49
164	272	7.30
165	273	6.93
166	274	6.45
167	275	6.08
168	276	5.52
169	277	5.68
170	278	5.50
171	279	5.18
172	280	5.27
173	281	5.62
174	282	5.51
175	283	5.76
176	284	5.74
177	285	6.01
178	286	5.89
179	287	6.43
180	288	6.25
181	289	6.24
182	290	5.83
183	291	5.59
184	292	5.02
185	293	4.02
186	294	3.31
187	295	2.62
188	296	0.01
189	297	0.83
190	298	0.70
191	299	0.40
192	300	0.85
193	301	1.22
194	302	1.49
195	303	1.86
196	304	2.23
197	305	2.59
198	306	2.72
199	307	2.93
200	308	3.03
201	309	3.34
202	310	3.45
203	311	3.47
204	312	3.43
205	313	3.38
206	314	3.22
207	315	3.23
208	316	3.18
209	317	3.32
210	318	3.41
211	319	3.65
212	320	3.64
213	321	3.78
214	322	3.69

Calculated Fission-Barrier Heights

N	A	B_{f} (MeV)
215	323	3.82
216	324	3.93
217	325	4.58
218	326	4.92
219	327	5.44
220	328	5.57
221	329	5.92
222	330	6.11
$Z = 109$ (Mt)		
144	253	1.59
145	254	1.96
146	255	2.37
147	256	2.76
148	257	3.22
149	258	3.58
150	259	4.20
151	260	4.65
152	261	5.13
153	262	5.48
154	263	5.70
155	264	5.91
156	265	5.88
157	266	5.88
158	267	6.04
159	268	6.28
160	269	6.70
161	270	7.14
162	271	7.49
163	272	7.68
164	273	7.41
165	274	7.11
166	275	6.59
167	276	6.16
168	277	5.63
169	278	5.44
170	279	5.31
171	280	5.47
172	281	5.48
173	282	5.79
174	283	5.88
175	284	6.30
176	285	6.22
177	286	6.51
178	287	6.51
179	288	6.96
180	289	6.56
181	290	6.51
182	291	6.10
183	292	5.86
184	293	5.26
185	294	4.38
186	295	3.78
187	296	3.06
188	297	2.24
189	298	1.12
190	299	0.06
191	300	0.13
192	301	0.07
193	302	0.83
194	303	1.15

Calculated Fission-Barrier Heights

N	A	B_{f} (MeV)
195	304	1.57
196	305	1.90
197	306	2.23
198	307	2.45
199	308	2.65
200	309	2.76
201	310	3.03
202	311	3.21
203	312	3.23
204	313	3.06
205	314	3.03
206	315	2.87
207	316	2.92
208	317	2.86
209	318	3.04
210	319	3.08
211	320	3.33
212	321	3.35
213	322	3.48
214	323	3.50
215	324	3.72
216	325	4.14
217	326	4.62
218	327	4.99
219	328	5.44
220	329	5.48
221	330	5.83
$Z = 110$ (Ds)		
146	256	1.76
147	257	2.12
148	258	2.68
149	259	3.15
150	260	3.70
151	261	4.17
152	262	4.68
153	263	4.99
154	264	5.27
155	265	5.35
156	266	5.34
157	267	5.47
158	268	5.48
159	269	5.95
160	270	6.45
161	271	6.92
162	272	7.31
163	273	7.48
164	274	7.27
165	275	6.90
166	276	6.49
167	277	6.09
168	278	5.59
169	279	5.64
170	280	5.69
171	281	5.86
172	282	5.94
173	283	6.46
174	284	6.70
175	285	7.25
176	286	7.26
177	287	7.45

Calculated Fission-Barrier Heights

N	A	B_{f} (MeV)
178	288	7.45
179	289	7.61
180	290	7.33
181	291	7.21
182	292	6.73
183	293	6.46
184	294	5.85
185	295	4.91
186	296	4.39
187	297	3.51
188	298	2.75
189	299	2.07
190	300	0.59
191	301	0.22
192	302	0.24
193	303	0.23
194	304	0.61
195	305	1.04
196	306	1.36
197	307	1.75
198	308	2.04
199	309	2.21
200	310	2.46
201	311	2.83
202	312	2.88
203	313	2.87
204	314	2.76
205	315	2.72
206	316	2.55
207	317	2.56
208	318	2.46
209	319	2.65
210	320	2.68
211	321	2.88
212	322	2.98
213	323	3.19
214	324	3.26
215	325	3.67
216	326	4.02
217	327	4.53
218	328	5.03
219	329	5.04
220	330	5.39
$Z = 111$ (Rg)		
148	259	2.32
149	260	2.71
150	261	3.20
151	262	3.62
152	263	4.21
153	264	4.42
154	265	4.75
155	266	4.72
156	267	4.80
157	268	4.88
158	269	5.10
159	270	5.70
160	271	6.13
161	272	6.62
162	273	6.96
163	274	7.20

Calculated Fission-Barrier Heights

N	A	$B_{\rm f}$ (MeV)
164	275	7.01
165	276	6.71
166	277	6.37
167	278	6.06
168	279	5.70
169	280	6.01
170	281	6.03
171	282	6.37
172	283	6.64
173	284	7.26
174	285	7.55
175	286	8.06
176	287	7.87
177	288	7.90
178	289	7.98
179	290	8.12
180	291	7.86
181	292	7.78
182	293	7.20
183	294	6.88
184	295	6.21
185	296	5.38
186	297	4.79
187	298	3.89
188	299	3.36
189	300	2.55
190	301	1.79
191	302	1.27
192	303	0.13
193	304	0.16
194	305	0.53
195	306	0.68
196	307	0.94
197	308	1.37
198	309	1.66
199	310	1.93
200	311	2.21
201	312	2.58
202	313	2.64
203	314	2.59
204	315	2.51
205	316	2.52
206	317	2.29
207	318	2.34
208	319	2.21
209	320	2.45
210	321	2.38
211	322	2.54
212	323	2.60
213	324	2.90
214	325	3.27
215	326	3.81
216	327	4.24
217	328	4.73
218	329	4.95
219	330	5.15
$Z = 112$ (Cn)		
150	262	2.65
151	263	3.15
152	264	3.61

Calculated Fission-Barrier Heights

N	A	B_{f} (MeV)
153	265	3.79
154	266	4.05
155	267	4.11
156	268	4.06
157	269	4.25
158	270	4.72
159	271	5.18
160	272	5.63
161	273	6.10
162	274	6.51
163	275	6.71
164	276	6.59
165	277	6.36
166	278	5.99
167	279	5.78
168	280	5.89
169	281	6.25
170	282	6.51
171	283	6.99
172	284	7.41
173	285	8.00
174	286	8.24
175	287	8.40
176	288	8.53
177	289	8.59
178	290	8.74
179	291	8.82
180	292	8.58
181	293	8.44
182	294	7.96
183	295	7.60
184	296	6.93
185	297	6.03
186	298	5.52
187	299	4.37
188	300	4.32
189	301	3.09
190	302	2.30
191	303	1.54
192	304	0.96
193	305	0.55
194	306	0.05
195	307	0.09
196	308	0.42
197	309	0.86
198	310	1.28
199	311	1.57
200	312	2.03
201	313	2.30
202	314	2.37
203	315	2.34
204	316	2.25
205	317	2.27
206	318	2.06
207	319	2.12
208	320	1.96
209	321	2.19
210	322	2.10
211	323	2.25
212	324	2.45

Calculated Fission-Barrier Heights

N	A	B_{f} (MeV)
213	325	2.77
214	326	3.04
215	327	3.56
216	328	4.10
217	329	4.54
218	330	4.76
$Z = 113$ (X)		
153	266	3.06
154	267	3.25
155	268	3.25
156	269	3.38
157	270	3.80
158	271	4.26
159	272	4.77
160	273	5.22
161	274	5.70
162	275	6.09
163	276	6.38
164	277	6.31
165	278	6.06
166	279	6.12
167	280	6.41
168	281	6.66
169	282	6.98
170	283	7.35
171	284	7.93
172	285	8.33
173	286	8.72
174	287	8.75
175	288	8.92
176	289	9.14
177	290	9.28
178	291	9.33
179	292	9.44
180	293	9.05
181	294	8.88
182	295	8.34
183	296	7.97
184	297	7.26
185	298	6.42
186	299	5.89
187	300	4.79
188	301	4.20
189	302	3.76
190	303	2.93
191	304	1.92
192	305	1.34
193	306	0.73
194	307	0.50
195	308	0.31
196	309	0.37
197	310	0.79
198	311	0.85
199	312	1.26
200	313	1.70
201	314	2.00
202	315	2.11
203	316	2.22
204	317	2.09
205	318	2.12

Calculated Fission-Barrier Heights

N	A	B_{f} (MeV)
206	319	1.91
207	320	1.95
208	321	1.80
209	322	1.96
210	323	1.86
211	324	2.02
212	325	2.24
213	326	2.60
214	327	2.88
215	328	3.43
216	329	3.91
217	330	4.26
$Z = 114$ (Fl)		
155	269	2.76
156	270	2.97
157	271	3.37
158	272	3.79
159	273	4.26
160	274	4.69
161	275	5.15
162	276	5.53
163	277	5.85
164	278	6.55
165	279	6.97
166	280	7.13
167	281	7.18
168	282	7.33
169	283	7.65
170	284	8.09
171	285	8.82
172	286	9.00
173	287	9.23
174	288	9.18
175	289	9.61
176	290	9.89
177	291	9.97
178	292	9.98
179	293	9.89
180	294	9.53
181	295	9.35
182	296	8.87
183	297	8.47
184	298	7.82
185	299	6.92
186	300	6.43
187	301	5.25
188	302	4.68
189	303	3.50
190	304	3.68
191	305	2.36
192	306	1.83
193	307	0.94
194	308	0.71
195	309	0.53
196	310	0.57
197	311	0.74
198	312	0.79
199	313	1.04
200	314	1.47
201	315	1.74

Calculated Fission-Barrier Heights

N	A	B_{f} (MeV)
202	316	1.92
203	317	1.97
204	318	1.91
205	319	1.85
206	320	1.46
207	321	1.45
208	322	1.32
209	323	1.53
210	324	1.63
211	325	1.72
212	326	2.05
213	327	2.40
214	328	2.75
215	329	3.17
216	330	3.50
$Z = 115$ (X)		
157	272	3.08
158	273	3.47
159	274	3.86
160	275	4.29
161	276	4.75
162	277	5.20
163	278	5.61
164	279	6.51
165	280	6.70
166	281	6.82
167	282	7.18
168	283	7.60
169	284	8.18
170	285	8.58
171	286	8.96
172	287	9.20
173	288	9.42
174	289	9.29
175	290	9.53
176	291	9.60
177	292	9.76
178	293	9.87
179	294	9.93
180	295	9.57
181	296	9.36
182	297	8.81
183	298	8.38
184	299	7.68
185	300	6.75
186	301	6.27
187	302	5.16
188	303	4.58
189	304	3.55
190	305	2.99
191	306	2.44
192	307	1.99
193	308	1.25
194	309	1.05
195	310	0.67
196	311	0.60
197	312	0.67
198	313	0.66
199	314	0.79
200	315	1.11

Calculated Fission-Barrier Heights

N	A	B_{f} (MeV)
201	316	1.42
202	317	1.65
203	318	1.62
204	319	1.50
205	320	1.38
206	321	1.01
207	322	0.81
208	323	0.85
209	324	1.24
210	325	1.51
211	326	1.58
212	327	1.76
213	328	2.10
214	329	2.50
215	330	3.08
$Z = 116$ (Lv)		
159	275	3.32
160	276	3.79
161	277	4.25
162	278	4.91
163	279	5.35
164	280	6.21
165	281	6.41
166	282	6.66
167	283	7.16
168	284	7.65
169	285	8.23
170	286	8.47
171	287	8.76
172	288	9.02
173	289	8.95
174	290	8.94
175	291	9.08
176	292	9.26
177	293	9.35
178	294	9.46
179	295	9.49
180	296	9.10
181	297	8.86
182	298	8.27
183	299	7.87
184	300	7.18
185	301	6.22
186	302	5.74
187	303	4.62
188	304	4.07
189	305	3.02
190	306	2.55
191	307	1.75
192	308	1.73
193	309	0.93
194	310	0.72
195	311	0.44
196	312	0.41
197	313	0.63
198	314	0.61
199	315	0.61
200	316	0.90
201	317	1.28
202	318	1.47

Calculated Fission-Barrier Heights

N	A	B_{f} (MeV)
203	319	1.36
204	320	1.16
205	321	1.09
206	322	0.63
207	323	0.53
208	324	0.63
209	325	0.97
210	326	1.24
211	327	1.29
212	328	1.50
213	329	1.84
214	330	2.20
$Z = 117$ (X)		
161	278	4.14
162	279	4.83
163	280	5.21
164	281	6.01
165	282	6.30
166	283	6.69
167	284	7.27
168	285	7.79
169	286	8.34
170	287	8.70
171	288	8.57
172	289	8.61
173	290	8.90
174	291	8.88
175	292	8.99
176	293	8.96
177	294	9.04
178	295	9.06
179	296	9.17
180	297	8.77
181	298	8.48
182	299	7.87
183	300	7.42
184	301	6.78
185	302	5.83
186	303	5.35
187	304	4.24
188	305	3.66
189	306	2.66
190	307	2.26
191	308	2.04
192	309	1.77
193	310	1.35
194	311	1.07
195	312	0.48
196	313	0.24
197	314	0.43
198	315	0.49
199	316	0.50
200	317	0.50
201	318	0.89
202	319	1.07
203	320	0.98
204	321	0.73
205	322	0.55
206	323	0.15
207	324	0.24

Calculated Fission-Barrier Heights

N	A	B_{f} (MeV)
208	325	0.25
209	326	0.65
210	327	0.79
211	328	1.10
212	329	1.15
213	330	1.50
$Z = 118$ (X)		
163	281	4.73
164	282	5.49
165	283	5.88
166	284	6.31
167	285	6.85
168	286	7.37
169	287	8.12
170	288	8.32
171	289	8.85
172	290	8.39
173	291	8.41
174	292	8.41
175	293	8.53
176	294	8.48
177	295	8.46
178	296	8.36
179	297	8.49
180	298	8.05
181	299	7.76
182	300	7.15
183	301	6.67
184	302	6.01
185	303	5.08
186	304	4.54
187	305	3.38
188	306	2.90
189	307	2.61
190	308	2.49
191	309	2.41
192	310	1.95
193	311	1.62
194	312	1.43
195	313	1.03
196	314	0.81
197	315	0.43
198	316	0.38
199	317	0.35
200	318	0.38
201	319	0.72
202	320	0.90
203	321	0.84
204	322	0.57
205	323	0.36
206	324	0.37
207	325	0.39
208	326	0.27
209	327	0.36
210	328	0.50
211	329	0.79
212	330	0.91
$Z = 119$ (X)		
165	284	5.51
166	285	6.19

Calculated Fission-Barrier Heights

N	A	B_{f} (MeV)
167	286	6.70
168	287	7.34
169	288	7.90
170	289	8.06
171	290	7.62
172	291	7.80
173	292	8.05
174	293	8.12
175	294	8.29
176	295	8.06
177	296	8.07
178	297	7.94
179	298	8.10
180	299	7.72
181	300	7.37
182	301	6.71
183	302	6.22
184	303	5.54
185	304	4.64
186	305	4.08
187	306	2.94
188	307	3.08
189	308	3.09
190	309	2.93
191	310	2.85
192	311	2.44
193	312	1.99
194	313	1.75
195	314	1.57
196	315	1.35
197	316	1.00
198	317	0.93
199	318	0.57
200	319	0.44
201	320	0.55
202	321	0.53
203	322	0.64
204	323	0.63
205	324	0.56
206	325	0.62
207	326	0.60
208	327	0.42
209	328	0.34
210	329	0.15
211	330	0.44
$Z = 120$ (X)		
167	287	6.35
168	288	6.85
169	289	7.35
170	290	7.70
171	291	8.26
172	292	7.36
173	293	7.44
174	294	7.57
175	295	7.71
176	296	7.69
177	297	7.54
178	298	7.33
179	299	7.48
180	300	7.01

Calculated Fission-Barrier Heights

N	A	B_{f} (MeV)
181	301	6.68
182	302	6.07
183	303	5.55
184	304	4.86
185	305	3.80
186	306	3.22
187	307	3.10
188	308	3.15
189	309	3.13
190	310	2.96
191	311	2.88
192	312	2.51
193	313	2.07
194	314	1.84
195	315	1.69
196	316	1.58
197	317	1.31
198	318	1.19
199	319	0.92
200	320	0.81
201	321	0.80
202	322	0.81
203	323	0.79
204	324	0.68
205	325	0.54
206	326	0.58
207	327	0.55
208	328	0.49
209	329	0.52
210	330	0.40
$Z = 121$ (X)		
169	290	7.07
170	291	6.46
171	292	6.82
172	293	6.89
173	294	7.31
174	295	7.03
175	296	7.19
176	297	7.16
177	298	7.05
178	299	6.99
179	300	7.10
180	301	6.66
181	302	6.31
182	303	5.64
183	304	5.11
184	305	4.40
185	306	3.38
186	307	2.62
187	308	2.90
188	309	2.96
189	310	2.92
190	311	2.75
191	312	2.72
192	313	2.35
193	314	1.97
194	315	1.74
195	316	1.51
196	317	1.45
197	318	1.36

Calculated Fission-Barrier Heights

N	A	B_{f} (MeV)
198	319	1.25
199	320	1.04
200	321	0.89
201	322	0.90
202	323	0.89
203	324	0.71
204	325	0.62
205	326	0.50
206	327	0.57
207	328	0.63
208	329	0.17
209	330	0.70
$Z = 122$ (X)		
172	294	6.32
173	295	6.54
174	296	6.53
175	297	6.31
176	298	6.33
177	299	6.28
178	300	6.19
179	301	6.23
180	302	5.60
181	303	5.51
182	304	4.87
183	305	4.33
184	306	3.62
185	307	2.60
186	308	1.82
187	309	2.45
188	310	2.41
189	311	2.38
190	312	2.26
191	313	2.25
192	314	1.82
193	315	1.54
194	316	1.46
195	317	1.18
196	318	1.18
197	319	1.02
198	320	0.95
199	321	0.74
200	322	0.77
201	323	0.74
202	324	0.66
203	325	0.48
204	326	0.46
205	327	0.35
206	328	0.38
207	329	0.49
208	330	0.41
$Z = 123$ (X)		
174	297	6.09
175	298	5.84
176	299	5.60
177	300	5.54
178	301	5.45
179	302	5.45
180	303	5.01
181	304	4.93
182	305	4.25

Calculated Fission-Barrier Heights

N	A	B_{f} (MeV)
183	306	3.69
184	307	2.95
185	308	1.94
186	309	1.14
187	310	2.10
188	311	2.01
189	312	1.90
190	313	1.81
191	314	1.81
192	315	1.38
193	316	1.36
194	317	1.31
195	318	1.01
196	319	0.82
197	320	0.63
198	321	0.53
199	322	0.48
200	323	0.60
201	324	0.58
202	325	0.57
203	326	0.45
204	327	0.35
205	328	0.29
206	329	0.33
207	330	0.46
$Z = 124$ (X)		
176	300	5.64
177	301	5.77
178	302	5.63
179	303	5.45
180	304	4.12
181	305	3.90
182	306	3.32
183	307	2.74
184	308	2.01
185	309	1.85
186	310	1.75
187	311	1.74
188	312	1.66
189	313	1.45
190	314	1.35
191	315	1.27
192	316	1.10
193	317	0.96
194	318	0.78
195	319	0.39
196	320	0.13
197	321	0.00
198	322	0.00
199	323	0.21
200	324	0.34
201	325	0.47
202	326	0.43
203	327	0.48
204	328	0.37
205	329	0.36
206	330	0.16
$Z = 125$ (X)		
178	303	5.64
179	304	5.45

Calculated Fission-Barrier Heights

N	A	B_{f} (MeV)
180	305	4.93
181	306	4.44
182	307	3.71
183	308	1.81
184	309	1.08
185	310	1.96
186	311	1.80
187	312	1.98
188	313	1.58
189	314	1.82
190	315	1.74
191	316	1.58
192	317	1.11
193	318	0.79
194	319	0.45
195	320	0.08
196	321	0.00
197	322	0.00
198	323	0.00
199	324	0.00
200	325	0.19
201	326	0.35
202	327	0.32
203	328	0.40
204	329	0.33
205	330	0.31
$Z = 126$ (X)		
180	306	4.69
181	307	4.09
182	308	3.51
183	309	2.60
184	310	1.80
185	311	2.08
186	312	1.87
187	313	1.85
188	314	1.75
189	315	2.01
190	316	1.84
191	317	1.67
192	318	1.17
193	319	0.91
194	320	0.36
195	321	0.00
196	322	0.00
197	323	0.00
198	324	0.00
199	325	0.00
200	326	0.00
201	327	0.13
202	328	0.26
203	329	0.47
204	330	0.51
$Z = 127$ (X)		
183	310	2.63
184	311	2.08
185	312	2.15
186	313	1.93
187	314	2.02
188	315	2.07
189	316	2.26

Calculated Fission-Barrier Heights

N	A	B_{f} (MeV)
190	317	2.05
191	318	1.56
192	319	1.11
193	320	1.00
194	321	0.47
195	322	0.12
196	323	0.00
197	324	0.00
198	325	0.00
199	326	0.00
200	327	0.00
201	328	0.00
202	329	0.11
203	330	0.39
$Z = 128$ (X)		
185	313	2.00
186	314	1.71
187	315	2.10
188	316	2.11
189	317	2.15
190	318	1.93
191	319	1.57
192	320	1.26
193	321	0.93
194	322	0.67
195	323	0.36
196	324	0.12
197	325	0.00
198	326	0.00
199	327	0.00
200	328	0.00
201	329	0.00
202	330	0.18
$Z = 129$ (X)		
187	316	2.05
188	317	2.01
189	318	1.93
190	319	1.81
191	320	1.59
192	321	1.31
193	322	1.12
194	323	0.90
195	324	0.50
196	325	0.24
197	326	0.00
198	327	0.00
199	328	0.00
200	329	0.00
201	330	0.00
$Z = 130$ (X)		
189	319	2.03
190	320	1.91
191	321	1.69
192	322	1.22
193	323	1.18
194	324	0.85
195	325	0.45
196	326	0.20
197	327	0.03
198	328	0.00

Calculated Fission-Barrier Heights

N	A	B_{f} (MeV)
199	329	0.00
200	330	0.00